

FINAL REPORT

Research project on
“A Study in Urban Air Pollution Improvement in Asia”

Submitted to JICA-Research Institute

Submitted by:

Prof. Nguyen Thi Kim Oanh

Asian Institute of Technology (AIT)

and the project team



October 2017

Content

EXECUTIVE SUMMARY	4
1. INTRODUCTION	6
2. RESEARCH METHODOLOGY	7
2.1 Sampling site description.....	7
2.2 Part 1: particulate matter monitoring.....	8
2.2.1 Sampling method.....	8
2.2.2 Sampling preparation and sample transport	9
2.2.3 Analytical methods	9
2.2.4 Quality assurance and quality control	10
2.2.5 Data analysis and source apportionment for PM.....	12
2.3 Part 2: acid deposition	12
2.3.1 Sampling method.....	12
2.3.2 Analytical methods	12
2.3.3 Data analysis.....	12
2.3.4 Secondary data collection.....	14
2.4 Part 3: PM _{2.5} air quality dispersion model.....	14
2.4.1 Emission inventory	14
2.4.2 WRF modeling	15
2.4.3 WRF/CAMx modeling	15
3. RESULTS AND DISCUSSION.....	17
3.1 Part 1: particulate matter monitoring results	17
3.1.1 PM Mass concentrations.....	17
3.1.2 Proportion of PM _{2.5} in SPM.....	21
3.1.3 BC and EC/OC	21
3.1.4 Ion concentration	22
3.1.5 Source apportionment using receptor modeling	25
3.2 Part 2: acid deposition.....	28
3.2.1 pH of rainwater.....	28
3.2.2 Monthly weighted average ionic concentrations in rainwater.....	29
3.2.3 Wet deposition flux	30
3.2.4 Atmospheric concentration of gaseous pollutants	31

3.2.6 Dry deposition fluxes.....	33
3.2.7 Total deposition amount.....	34
3.3 Part 3: PM air quality dispersion model	38
3.3.1 Emission inventory for base year of 2015	38
3.3.2 WRF model performance evaluation.....	40
3.3.3 CAMx model performance evaluation	41
3.3.4 Simulated fields of PM _{2.5} in BMR.....	43
4. CONCLUSION AND RECOMMENDATION	46
4.1 Summary and Conclusions	46
4.1.1 Particulate matter mass and compositions.....	46
4.1.2 Source apportionment results	47
4.1.3 Acid deposition.....	47
4.1.4 Emission inventory and PM air quality dispersion modeling.....	47
4.2 Recommendation	48
5. REFERENCE	50
APPENDICES	51

EXECUTIVE SUMMARY

This final report of the joint research project “A study in urban air pollution improvement in Asia” is submitted by the Asian Institute of Technology (AIT) on behalf of the project team following the contract between AIT and the Japan International Cooperation Agency (JICA) for the project period of March 2015 - December 2017. Technical support is provided by the Asia Center for Air Pollution Research (ACAP) Japan and the operational support is provided by the Pollution Control Department (PCD) of Thailand. The project aims at characterizing the particulate matter (PM) level and composition, ambient concentrations of acidic gases, as well as the ionic components of rainwater at two sites in the Bangkok Metropolitan Region (BMR): AIT (Pathumthani) and PCD (Bangkok). During the sampling period of September 2015 - February 2017, 78 weekly samples were collected for PM and acid gases (filter pack samplers) and rainwater (automatic wet-only collectors), respectively. The PM mass and ionic compositions were analyzed by AIT while the EC/OC were analyzed by ACAP. The sampling and analysis were done strictly following the required QA/QC procedure introduced by ACAP. The source apportionment study for PM_{2.5} measured at the sites was done using receptor models (the Chemical Mass Balance (CMB) Model and the Positive Matrix Factorization (PMF) Model). An emission inventory of PM and precursors was conducted for the BMR for the base year 2015 and the data were used to run a three-dimensional air quality modeling system of Weather Research Forecast – Comprehensive Air Quality Model with Extensions (WRF-CAMx) to simulate PM in BMR for August and November 2015. The simulation results were evaluated using the monitoring data.

In the dry period, the average fine (PM_{2.5}) and coarse (PM_{>2.5}) concentrations at AIT (32 ± 11 and $44 \pm 18 \mu\text{g}/\text{m}^3$) were higher than PCD (28 ± 10 and $41 \pm 15 \mu\text{g}/\text{m}^3$) while in the wet period, the levels at the two sites were close, i.e. $15 \pm 11 \mu\text{g}/\text{m}^3$ and $37 \pm 18 \mu\text{g}/\text{m}^3$ at AIT and $15 \pm 6 \mu\text{g}/\text{m}^3$ and $38 \pm 17 \mu\text{g}/\text{m}^3$ at PCD. At both sites, PM_{2.5} mass contributed more to the total suspended particulate matter (SPM = PM_{2.5} + PM_{>2.5}) in the dry period, about 42-43%, than in the wet period (30-31%). The average EC and OC levels in PM_{2.5} measured at AIT ($3.60 \pm 2.19 \mu\text{g}/\text{m}^3$ and $5.52 \pm 4.59 \mu\text{g}/\text{m}^3$, respectively) were higher than those at PCD ($2.75 \pm 1.44 \mu\text{g}/\text{m}^3$ and $4.29 \pm 3.34 \mu\text{g}/\text{m}^3$, respectively). The EC and OC in the coarse fraction (PM_{>2.5}) at AIT were $1.07 \pm 0.57 \mu\text{g}/\text{m}^3$ and $2.40 \pm 1.97 \mu\text{g}/\text{m}^3$, respectively, that were also higher than the corresponding levels measured at PCD, $0.84 \pm 0.55 \mu\text{g}/\text{m}^3$ and $1.80 \pm 0.67 \mu\text{g}/\text{m}^3$.

At both sites, the most dominant anion species in PM_{2.5} was SO₄²⁻ in both periods, i.e. the average levels at AIT for the wet and dry period were $2.37 \mu\text{g}/\text{m}^3$ and $4.10 \mu\text{g}/\text{m}^3$, respectively, while the corresponding values at PCD were $2.49 \mu\text{g}/\text{m}^3$ and $3.22 \mu\text{g}/\text{m}^3$, respectively. NH₄⁺ was the major cation in PM_{2.5} at both sites that contributed $1.55 \mu\text{g}/\text{m}^3$ and $0.78 \mu\text{g}/\text{m}^3$ at AIT, in wet and dry period, respectively, while corresponding levels at PCD were $0.79 \mu\text{g}/\text{m}^3$ and $1.41 \mu\text{g}/\text{m}^3$. The source apportionment (CMB) results showed that the major contributing sources to PM_{2.5} in both sites were traffic (diesel vehicles) and biomass open burning (OB) but their relative contributions varied with season. During the dry period higher relative contributions from biomass OB (38% at AIT and 35% at PCD) were obtained

as compared to the wet period (24.9% at AIT and 24.6% at PCD). The opposite was for the traffic contribution that was higher during the wet period (29% at AIT and 26% at PCD) than the dry period (27% at AIT and 21% at PCD) which may be explained by more intensive OB in BMR during the dry period. The full data set of PM_{2.5} compositions at the sites should be scrutinized to improve the source apportionment also by using the multivariate statistical model of PMF. Back trajectory (HYSPLIT) analyses showed that the weeks with high PM in BMR were normally characterized by the stagnant regional pathway of air mass while low PM period weeks were generally associated with the marine pathway of air mass.

Average pH of rainwater at AIT and PCD were 4.7 – 7.0 and 4.6 – 7.1, respectively, with the lower values recorded for the dry period and higher values were for the wet period. The average electrical conductivity of rainwater was 2.08 ± 1.65 mS/m for AIT and 2.02 ± 1.11 mS/m for PCD. The total annual wet deposition fluxes for different species at both sites ranged from 5.3 to 86.1 meq/m² with the following rank: $\text{NH}_4^+ > \text{Ca}_2^+ > \text{NO}_3^- > \text{SO}_4^{2-} > \text{Cl}^- > \text{Na}^+ > \text{K}^+ > \text{Mg}^{2+}$. The concentrations of acidic gases measured at both sites ranged from 0.6 to 13.5 ppb following the rank of $\text{NH}_3 > \text{SO}_2 > \text{HNO}_3 > \text{HCl}$. The dry deposition was calculated and the results were well below those of the wet deposition fluxes, especially during the rainy months. This implied that the wet deposition played an important role to remove sulfur (S) and nitrogen (N) species from the BMR atmosphere. The total sulfur deposition in 2016 was estimated at 586 kg/km²/yr while that of nitrogen was 2,235 kg/km²/yr which were still lower than the critical loads suggesting a low potential risk for the terrestrial ecosystem in Pathumthani at present.

Emission inventory results showed that on-road transport contributed the most to the total emissions of NO_x, CO, NMVOC, PM₁₀, PM_{2.5}, BC and OC (37 - 65%), while NH₃ emission was mainly from livestock (55%) and SO₂ was mainly from industry (90%). WRF simulation results were evaluated using the observations at two airports in BMR and the results showed satisfactory performance for temperature and relative humidity, but not for wind speed and wind direction. CAMx simulation results of PM_{2.5} showed higher concentrations in the city center for all months which also reflected the contributions from the traffic emissions. The CAMx could not capture the hourly PM_{2.5} recorded at three available PCD monitoring stations for both August and November. However, the comparison between CAMx simulated and weekly PM monitoring results obtained in this project showed more reasonable agreement.

A better characterization of PM in BMR requires a long-term monitoring period. The findings suggest that the traffic and biomass OB are the key sources contributing to PM; however PM mass and composition data collected over a longer period would provide better source apportionment results by using more advanced receptor models, such as PMF. The model simulation for PM should be conducted for the entire year to capture the seasonal variation and modelling tools should be applied to assess impacts of emission reduction scenarios on air quality and health as well as the co-benefit to the climate forcing reduction. The results of this project provide the scientific evidence to policy making toward better air quality in BMR.

1. INTRODUCTION

Urban air pollution has become a salient environmental issue in many Asian countries due to their rapid industrial development, urbanization, and motorization. Particulate matter (PM) pollution, such as PM_{2.5}, is of concern due to health and climate change impact. Bangkok is an example of Asian developing megacity that has PM pollution problem. Annual average concentration of PM₁₀ has been observed to be twice as high as those in most North American cities (Ostro et al, 1999). Thailand Pollution Control Department (PCD) has started routine monitoring for PM_{2.5} in Bangkok since 2010, after the standard was made effective. It is evident that a 10 µg/m³ change in daily PM₁₀ would be associated with a 1–2% increase in natural mortality, 1–2% increase in cardiovascular mortality, and a 3–6% increase in respiratory mortality (Ostro et al, 1999 and Vichit-Vadakan et al., 2010). In addition, the city also has been facing problem with acid rain where acidity of rain water was reported to increase (EANET, 2015).

Mitigation measures to reduce PM pollution in the city are urgently required. However, to design appropriate policies, the government needs information of major contributing sources of PM which in turn requires detail analyses of PM composition over a long period. Simultaneously monitored levels of the acidic gases as well as acidic components of the rain water would help to explain the formation and removal processes of PM. The deposition of these acidic substances, both in wet and dry deposition fluxes, can be used to assess potential impacts on the ecosystem. This joint research project of “A study in urban air pollution improvement in Asia” is implemented by the Asian Institute of Technology (AIT) following the contract between AIT and the Japan International Cooperation Agency (JICA) for the project period of March 2015 - December 2017. Technical support is provided by the Asia Center for Air Pollution Research (ACAP) Japan and the operational support is provided by the Pollution Control Department (PCD) of Thailand. The project is supported by the national research counterparts including the Environmental Research and Training Center (ERTC), and King Mongkut’s University of Technology Thonburi (KMUTT) and Ladkrabang (KMITL).

The main objectives of the project as included in the contract are:

- (1) Perform sampling of PM_{2.5} at selected sites in Bangkok over a year and analyse its chemical compositions.
- (2) Estimation of seasonal variations of PM_{2.5} and its components at selected sites in Bangkok.
- (3) Model development and simulations (a receptor model and/or a chemical transport model) to identify the sources of PM_{2.5} in Bangkok.

In addition to the above-mentioned objectives the project activities also included monitoring of acidic components in rain water and ambient levels of acidic gases.

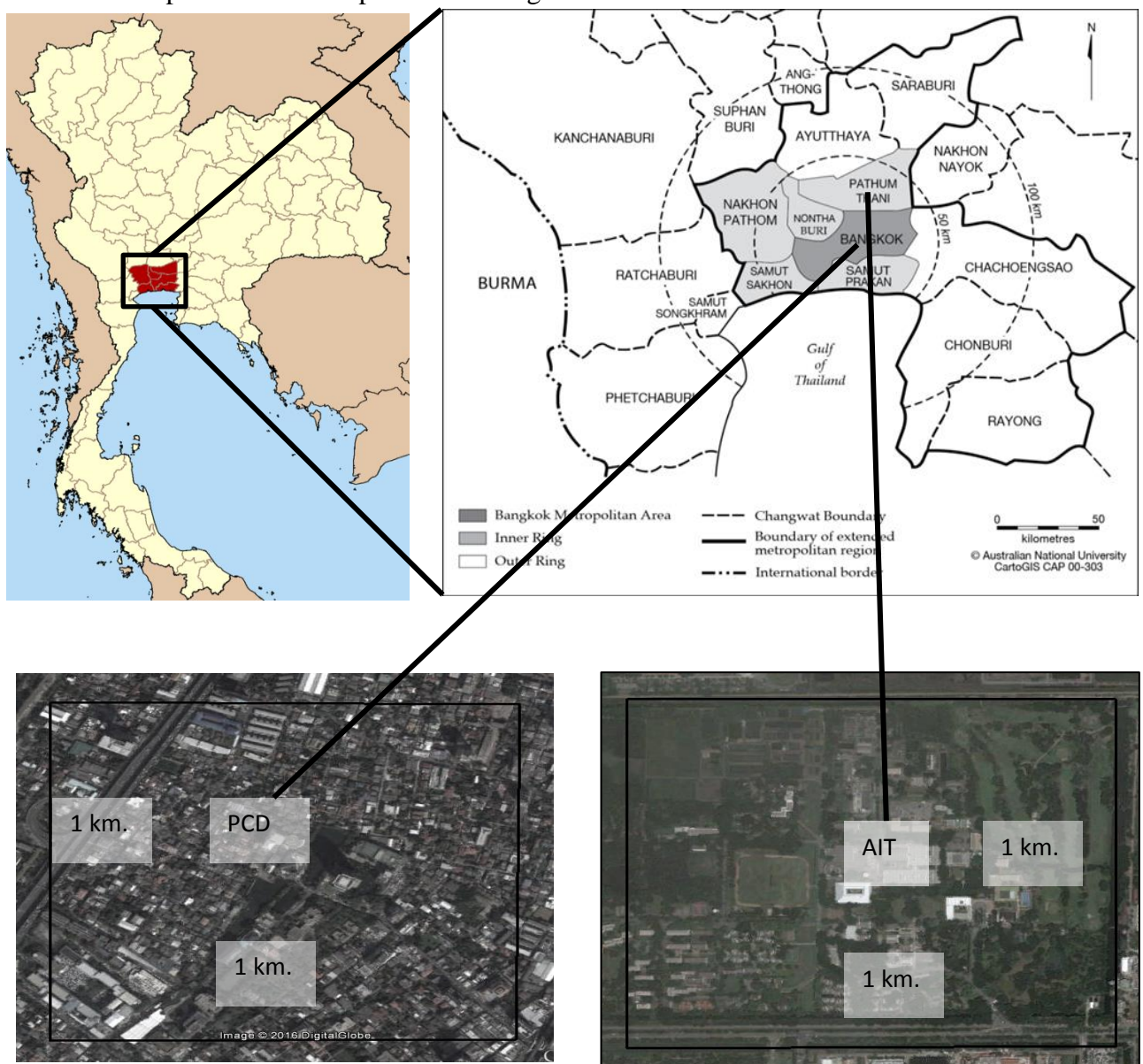
The project period is from March 2015 to December 2017 and this final report covered project activities (i.e. monitoring and modeling) conducted during the period of March 2015 – October 2017. For PM monitoring, the results for the period of September 2015 – February 2017 are reported.

2. RESEARCH METHODOLOGY

There are three (3) major research components in this study: 1) PM monitoring and assessment, 2) acid deposition monitoring, and 3) Emission inventory and PM dispersion modeling. Accordingly, the research methodology is summarized in the following section.

2.1 Sampling site description

Two sampling sites were rigorously selected mainly to represent urban and sub-urban area of Bangkok. One is located at the rooftop of the Pollution Control Department (PCD), Bangkok (urban) and the other is at the rooftop of the ambient laboratory of AIT (sub-urban). The orientation map of both sites is presented in Figure 1.



Source: Malulee (2015)

Figure 1 Monitoring sites at PCD and AIT

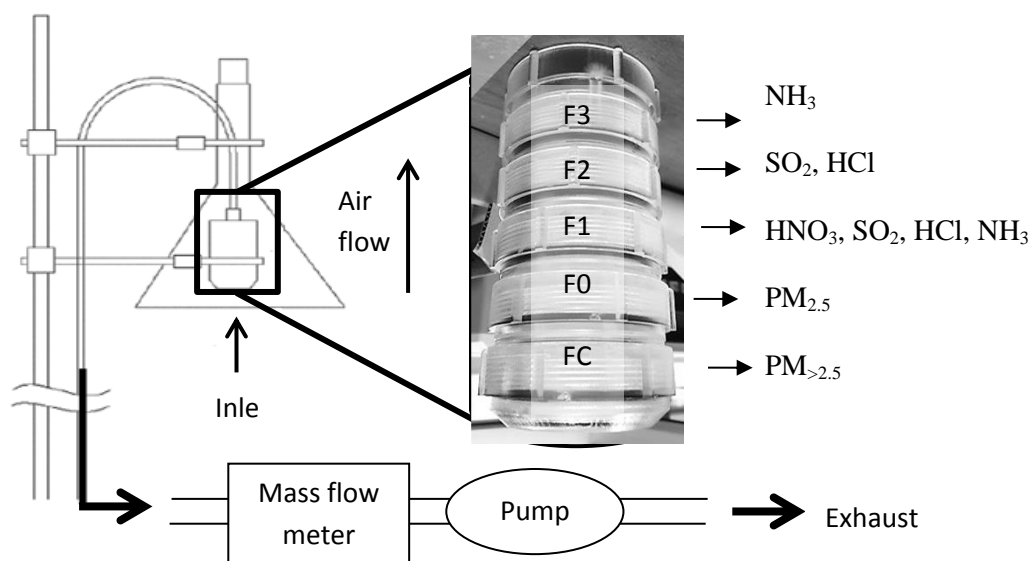
The characteristics and locations of two sampling sites are as described follows:

1. The rooftop of PCD building is located at 13.8° (N) and 100.5° (E) that is situated of 64 meters high above the ground. The building is mainly surrounded by houses, commercial places, and institutions within a radius of 5 Km. It is approximately located of 0.75 km away from the main road (Paholyothin, Rd) which has heavy traffic congestion during rush hours. Sky train line is located above this road.
2. Ambient laboratory at AIT, Pathumthani is located at 14.1° (N) and 100.6° (E) that is located 6 meters above the ground. This site is surrounded by many canals, rice paddies and other crops fields, as well as some small and medium industries. A mixed industrial estate is located about 8 km to the North (Navanakhon Industrial Estate) and the other was about 6 km to the South (Thai industry). AIT is located approximately 500 m away from the main road (Paholyothin, Rd) and is about 40 km from the Bangkok center. It is situated at the upwind of the Bangkok city during the dry season.

2.2 Part 1: particulate matter monitoring

2.2.1 Sampling method

The five-stage and two-stage filter pack air samplers were used to collect weekly ambient air samples, i.e. coarse particles ($PM_{>2.5}$) and fine particles ($PM_{2.5}$). The five-stage filter pack collected air samples on two types of filters: quartz filter (FC) for the coarse PM and Teflon filter (F0) for the fine PM. Weekly sampling was done from September 2015 to February 2017. The sampling pump was set at 2 L/min continuously over one-week sampling period (ACAP, 2015) using a mass flow controller. The samples were analysed for mass, ions and BC by AIT, and EC/OC (two-stage filter pack) by ACAP. A schematic picture of filter pack is presented in Figure 2. In parallel, a 2-stage filter pack was used with quartz filters which were sent to ACAP for EC/OC analysis. A summary of the monitoring with total number of samples, and number of valid samples are presented in Table 1.



Source: adapted from ACAP (2015)

Figure 2 Schematic diagram of the five-stage filter pack used in this project

Table 1 Summary of the Overall Monitoring Samples

Study period	Sampling site	Filter type	Number of sample (weekly)	Total number of sample	Total number of valid sample
September 2015 to February 2017	The rooftop of PCD building	Quartz filter (FC)	1	78	74
		Teflon filter (F0)	1	78	71
	AIT ambient laboratory	Quartz filter (FC)	1	78	74
		Teflon filter (F0)	1	78	71

2.2.2 Sampling preparation and sample transport

Leak check for the filter packs was conducted before shipping to the sampling sites. The filter packs were sealed with parafilms then covered by a polyethylene bag or sealed them with aluminium foil. The packs were kept in plastic zip lock bag before and after the sampling. Before sampling, filters for mass were conditioned (22 ± 2 °C and $40 \pm 5\%$ for 24h) and the pre-weight was recorded using a microbalance. The filter holder (with filters) was sealed into a polyethylene bag and further an aluminum-coated bag for avoiding the contamination and sunlight. The sealed mounted holder was kept in an icy box at approximately 10°C during shipping to a monitoring site to avoid evaporation of the substances. After sampling each sampled filter was kept in a Petri dish that was wrapped in airtight plastic bag and the whole bag was refrigerated until analysis.

2.2.3 Analytical methods

Quartz filters and Teflon filters were used to analyse for mass, ion components (SO_4^{2-} , NO_3^- , Cl^- , NH_4^+ , Na^+ , K^+ , Ca^{2+} , Mg^{2+}) and BC concentrations by AIT. The results of weekly concentrations of each composition were reported for coarse and fine fractions, separately. The filter weighing was done using a microbalance at Environmental Engineering Laboratory, King Mongkut's University of Technology Thonburi (KMUTT). The ions were analysed by IC at ERTC while BC measurement was done using OT21 at AIT. The seven points of standard curve were prepared from 0.02 ppm to the maximum standard concentration of 10 ppm of all ions. All of the standards curves for both cation and anion had R^2 larger than 0.99 with linear regressions except a cubic regression line only for Ammonium ion (Appendix 1).

Table 2 presents a summary of analytical methods used. In addition, in the source apportionment (section 2.2.5), this study also used EC/OC results produced by ACAP using the Thermal Optical Reflectance (TOR) method and elements results for both fine and coarse PM collected on 2 stage filter pack (quartz filters).

Table 2 Summary of Analytical Methods

PM and filter types	Parameter	Analytical method
Coarse particles (PM _{>2.5}): Quartz filter	Mass concentration	Gravimetric method by microbalance (7 digits)
	Ionic species (i.e. SO ₄ ²⁻ , NO ₃ ⁻ , Cl ⁻ , NH ₄ ⁺ , Na ⁺ , K ⁺ , Ca ²⁺ , Mg ²⁺)	Ion Chromatography (IC)
Fine particles (PM _{2.5}): Teflon filter	Mass concentration	Gravimetric method by microbalance (7 digits)
	Ionic species (i.e. SO ₄ ²⁻ , NO ₃ ⁻ , Cl ⁻ , NH ₄ ⁺ , Na ⁺ , K ⁺ , Ca ²⁺ , Mg ²⁺)	Ion Chromatography (IC)
	BC	OT21

2.2.4 Quality assurance and quality control

In order to ensure the data quality, the quality assurance and quality control (QA/QC) procedure was implemented throughout the sampling and analysis. Before analysis, the invalid samples were discarded. These were the samples taken when a filter pack stopped accidentally, for example when mass flow pump was automatically stopped or when the electricity was shut off. The filters would absorb gases when pump stopped and acted like passive samples hence causing bias.

For the analytical blanks, two types of filter blanks were used, i.e. trip blanks and lab blanks. Three blank filters were taken from each new filter lot, 1 per every 20 filters, and a lab blank value was determined as the median of the analytical results of the blank filters. For each month sampling, one blank value (one median value) was used for the weekly samples collected in the month. Trip blanks were used in order to determine any contamination occurred during the sample shipping. All filter blanks were stored in the same conditions and analysed using the same method with other actual sample filters. The results reported here were all blank corrected.

For mass determination, a lab blank was used to check the weight change every time the weighing was done. US EPA (1998) criteria is that the weight change in the blank should be below 15 µg otherwise the conditioning environment may be contaminated. If the filter blank gains more than 30 µg between pre and post sampling, all the filters of the lot with that filter blank is discarded. The electrostatic charge on the filters is removed by exposing the filters to a low level radioactive source (500 picocuries of Polonium²¹⁰) prior to and during the sample weighting. In this project the weighing was done following this QA/QC. Each filter was weighted at least three times or until the constant mass was obtained (Kim Oanh et al, 2014).

In this study, careful measures were taken to avoid problems occurring during filter weighing: (i) properly remove electrostatic charge on filters especially on PTFE filter (as it is the main cause of fluctuation of mass, i.e. more than 15 µg/filter blank) by exposing the

filters to anti-static strip over a longer period of time, (ii) recover all pieces of sampled Quartz filters because the fragile quartz may lose some materials during sample recovery.

For BC measurement, only Teflon filters (F0) was measured by OT21 at AIT laboratory. The empirical relation for samples collected on Teflon requires that quartz-fiber filters be placed underneath the Teflon filters in both 'Sample' and 'Reference' positions, to act as optical diffusers. In parallel the measurements were also done for Quartz filter pack for comparison with EC/OC results.

QA/QC for ions analysis included the preparation of the calibration curves using 9 data points for each analyte with the coefficient of determination (R^2) of greater than 0.99. Ion balance (R_1) check was done for both fine and coarse PM fractions.

2.2.5 Data analysis and source apportionment for PM

The composition of weekly samples of ions, elements (provided by ACAP), BC and EC/OC were compiled and the reconstructed mass was done using 8 mass groups (Kim Oanh et al., 2006) to preliminarily identify the major source factors of fine and coarse PM in each site. The ambient concentration data were prepared to include the measurement uncertainties in the input format required for receptor modelling.

Two receptor models were used to investigate major contributing sources to $PM_{2.5}$ in the 2 sites of BMR:

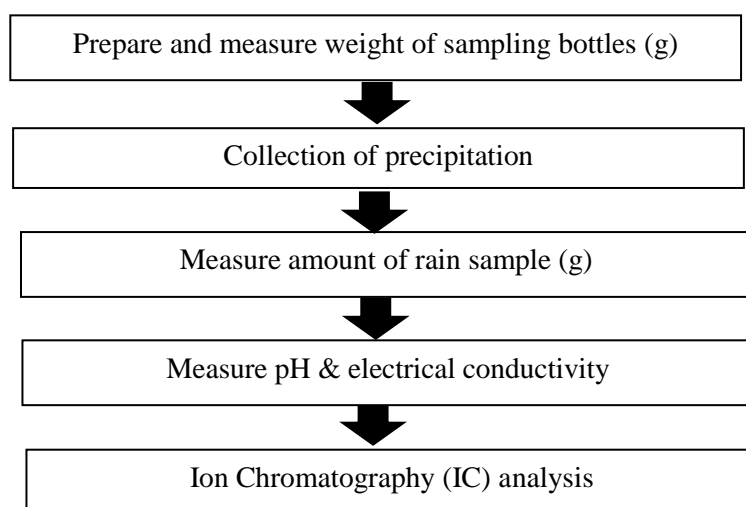
- a) Chemical Mass Balance (CMB) version 8.2 was used to quantify source contribution in this study. Moreover, this receptor model was the newest version which was available for download from http://www.epa.gov/scram001/receptor_cmb.html. In this study, source profiles were taken from Kim Oanh et al. (2013). Uncertainty was calculated using the equations provided in Kim Oanh et al. (2009) based on the split sample analyses done at AIT.
- b) Positive Matrix Factorization (PMF) model was used in this study by utilizing the input of PM concentration file and uncertainty file (prepared separately). The main results of the PMF are source contribution matrix (G factor) and source profile (F factor). Preliminary results are reported in this final report for PCD site only and were compared with the CMB results.

The receptor modeling results were evaluated using the current knowledge on the local sources and potential long-range transport (air mass trajectory) of air pollution to the 2 sites to provide more insight into the PM air pollution in BMR. The HYSPLIT model was run online (<http://ready.arl.noaa.gov/HYSPLIT.php>). The backward trajectories for selected sampling weeks in both wet and dry period were calculated starting from the sampling site coordinates, initiated at 0:00 UTC (UK) or +7GMT for Thailand at 500 m above the ground level. Meteorological input data were taken from the Global Data Assimilation System (GDAS) provided in the website. The weeks with the highest and lowest mass concentrations were chosen to examine the possibility of the long-range transport pollutants effecting PM level at the sites.

2.3 Part 2: acid deposition

2.3.1 Sampling method

The 5-stage filter pack (Figure 2) collected gaseous compounds in F1, F2 and F3 stage. The polyamide filter for F1 stage was used to collect gases of SO₂, HNO₃, HCl and NH₃. F2-stage filter used for additional collecting of SO₂ and HCl was made of cellulose filter impregnated with an alkali solution. The F3-stage filter was made of cellulose filter impregnated with an acidic to additionally collect NH₃ (see Figure 2). An automated wet-only collector was used to collect rainwater at each site. The sampling procedure is shown in Figure 3.



Source: Adapted from EANET (2010)

Figure 3 Flow chart of wet deposition sampling

2.3.2 Analytical methods

After sampling, the filters of F1, F2 and F3 were extracted by solvent (Table 3) with shaking over 1 hour on an automatic shaker. The extraction method followed the procedure given in EANET (2010).

Table 3 Analytical Species and Solvent for F1, F2 and F3 (EANET, 2013)

Stage	Specifications of filters	Species	Solvents
F1	Nylon (Polyamide) filter	SO ₄ ²⁻ , NO ₃ ⁻ , Cl ⁻ , NH ₄ ⁺	MiliQ water
F2	Alkali (K ₂ CO ₃) impregnated cellulose	SO ₄ ²⁻ , Cl ⁻	0.05% H ₂ O ₂
F3	Acid (phosphoric acid) impregnated cellulose	NH ₄ ⁺	MiliQ water

2.3.3 Data analysis

a) Determination of rain sample concentration for wet deposition

The concentrations of components in rainwater and gaseous concentrations were first determined. The results were used to calculate weighted average concentrations of components in rain water, the dry deposition samples, and the total deposition flux following the EANET methods (EANET, 2010) as detailed in Appendix 2. This study applied a calculation program in Microsoft EXCEL provided by EANET (2010) to calculate the dry deposition velocity and dry deposition flux using the resistance method. Further, the total atmospheric deposition flux of S and N (in meq) were calculated for both sites by summing up the wet and dry deposition.

2.3.4 Quality assurance and quality control

a. Sample transport and storage

During transport, the sampled packs were placed in an icy box, the same as for the PM samples described above. The samples (filter packs and rainwater samples) were stored at 5°C at the Environmental Engineering and Management (EEM) laboratory at AIT prior to analysis.

b. Blanks

Three filters from each filter lot were analysed as laboratory blanks. The median value of three blank filters was used as blank value (EANET, 2013).

c. Ion chromatography

The extraction procedure was done following ACAP standard operating procedure (ACAP, 2015). The calibration curves were prepared for each analyte using 9 data points with R^2 of more than 0.99.

d. Ion balance (R1)

The principle of electro-neutrality in precipitation requires that the total anion equivalents are equal the total cation equivalents. According to this principle, ion balance in precipitation samples was checked by the method described in EANET (2010). Calculated R1 should principally meet the criteria provided by EANET (2010).

e. Electrical conductivity balance (R2)

The total electrical conductivity was calculated in mS/m from the molar concentrations and molar conductivity of individual ions. The observed electrical conductivity values were checked by the method described in EANET (2010). Calculated R2 should principally meet the criteria provided by the EANET manual (EANET, 2010).

f. Accuracy of chemical analysis

Artificial precipitation inter-calibration samples were provided by ACAP and were used to check with our analytical results to ensure the value accuracy. In principle, the results of these inter-calibrations were used to analyse the existing laboratory problems and to improve

the quality of laboratory analyses (EANET, 2010). The measured values should be within the acceptable range of $\pm 15\%$.

2.3.4 Secondary data collection

a. Meteorological data

Wind speed (m/s), temperature ($^{\circ}\text{C}$), precipitation amount (mm), relative humidity (%), cloud coverage and solar radiation (W/m^2) are required parameters to calculate the dry deposition velocity. For PCD site meteorological data was collected from the Don Mueang (DNM) airport station (located within a distance of 15 km from PCD). Pathumthani agrometeorological station meteorological data was collected to calculate the dry deposition at AIT (located within a distance of 4 km). Solar radiation data was taken from the measurements taken by the AIT energy laboratory to cover the whole study period from September 2015 to February 2017. The collected data is presented in Appendix 2.2.

b. Land use and land coverage

Land use and land cover data were collected from the Land Development (TLD) Department of Thailand for calculation of dry deposition velocity that was required for estimation of the dry deposition fluxes and determination of critical loads of the ecosystem. The types of land use considered are tree cover (forest as termed in the EANET software), grass, agricultural, water, and building & road surfaces. Both sampling sites were categorized as mixed land use.

2.3.5 Assessment of potential impact of acid deposition

The comparison between the results of total deposition fluxes obtained in this study with the available critical load values was done to assess the potential impacts of acid deposition on the terrestrial ecosystem in the Pathumthani province. Existing critical load values of sulfur and nitrogen for the study area were taken from relevant published sources (Milindekha, 2011); Bouwman and van Vuuren, 1999).

2.4 Part 3: $\text{PM}_{2.5}$ air quality dispersion model

2.4.1 Emission inventory

The available emission inventory (EI) for PM air quality simulation in BMR was updated to the base year of 2015. The on-road emission was updated using the driving pattern and emission factors generated from the International Vehicle Emission (IVE) model (Buadee, 2017). The biogenic emission was estimated using the Global Biosphere Emissions and Interactions System (GLOBEIS) model with an updated land use map. GLOBEIS model required gridded land-use data of BMR and gridded meteorological parameters (i.e. temperature and solar radiation) generated by WRF model. Industrial emission of 2013 was provided by Dr. Narisara Thongboonchoo (King Mongkuth University for Technology Ladkrabang, KMITL). Other sources were also updated by using the activity data for the year of 2015, such as for open burning (OB) of crop residue and municipal solid waste, residential combustion, fuel stations and livestock (Pornsiri, 2017). Emission factors (EFs) for the

above-mentioned sources were obtained from the compiled values by the Atmospheric Brown Cloud Emission Inventory Manual (ABC EIM) (Shrestha et al., 2013).

Monthly emissions for August and November 2015 were obtained directly from the activity data while hourly emissions were constructed using the hourly profiles for sources in BMR developed under the AIT-PTT Project (Kim Oanh et al., 2014). VOC (CB-IV species) and PM speciations were done using the profiles compiled by Pornsiri (2017) from various data sources. Emissions were further converted to model ready input format (in binary) using a Fortran program developed by the AIT team.

2.4.2 WRF modeling

Input data for Weather Research Forecast (WRF) model was the NCEP Final Analysis Data Operational Model Global Tropospheric Analyses (FNL) of 1-degree resolution operationally prepared, available every six hours, which was downloaded from the Data Support Section of the Computational and Information Systems Laboratory at the National Center for Atmospheric Research (NCAR) (<http://rda.ucar.edu/datasets/ds083.2>). The coarsest WRF domain (WRF d1) comprised of 96×99 horizontal grid cells with a grid resolution of 18 km, the middle WRF domain (WRF d2) comprised of 81×81 horizontal grid cells with grid resolution of 6 km and the inner-most WRF domain comprised of 50×50 horizontal grid cells with grid resolution of 2 km (Figure 4). The vertical structure of WRF domain consisted of 30 sigma layers, ranging from the ground surface level to the top of 15.797 km.

The evaluation of WRF performance was done by comparing WRF outputs (i.e. hourly temperature, relative humidity, wind speed and direction) with the observations from 2 airports, Survanabhumi (SVN) and DNM. The statistical measures used to evaluate the meteorological model performance included mean bias (MB), the mean absolute gross error (MAGE), the root mean squared error (RMSE) and the calculated values were compared with the criteria provided by Emery et al. (2001).

2.4.3 WRF/CAMx modeling

Particulate matter air quality in the BMR domain was simulated using 3D chemical transport model of the Comprehensive Air Quality Model with Extensions (CAMx) with meteorological fields driven by the WRF for two months: August and November 2015. This study applied two-way nesting domains for photochemical grid model (PGM) with the coarse domain being the Central of Thailand (CENTHAI) domain (PGM d1). PGM d1 covers the central area of Thailand and some parts of the gulf of Thailand with an area of 300×300 km² consisting of 50×50 horizontal grid cells with a grid resolution of 6 km (Figure 4). The fine domain is the BMR domain (PGM d2) which had an area of 70×100 km² covering Bangkok and nine provinces. CAMx domain consisted of 15 layers to match the layer interface of WRF. The model system was run on PC/Linux platform using the computer lab at the Environmental Engineering and Management Program, AIT. The initial and boundary conditions for CAMx CENTHAI domain were extracted from the study of Permadi (2013) who simulated air quality for whole Southeast Asia domain using regional CTM of CHIMERE/WRF.

CAMx results for hourly PM_{2.5} and PM₁₀ concentrations were compared with the data obtained from the PCD automatic monitoring stations. The weekly concentrations and compositions obtained in the monitoring part of this JICA PM_{2.5} project at AIT and PCD sites were used to compare with the weekly modelling outputs. For PM simulation evaluation, the

Mean fractional bias (MFB) and mean fractional error (MFE) values were calculated and were compared with the criteria provided by Boylan and Russel (2006).

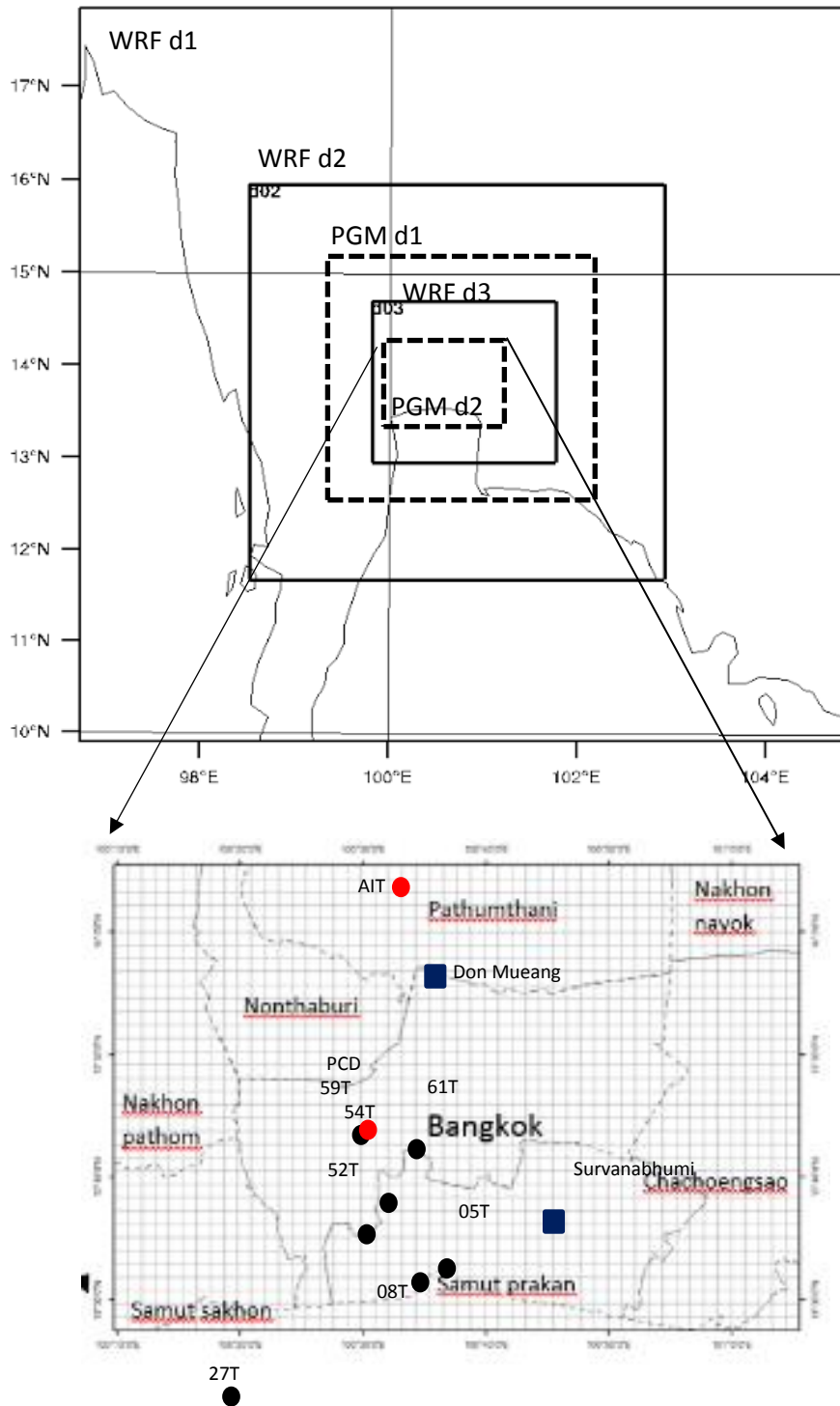


Figure 4 WRF and CAMx modeling domains and ground monitoring stations

Note: AIT: JICA sites: Asian Institute of Technology (AIT), and Pollution Control Department (PCD). PCD automatic monitoring stations: 05T (Bangna), 08T (Phra Pradaeng), 27T (Samut Sakhon), 52T(Thonburi), 54T (Din Daeng), 59T (Government public relation department), and 61T (Wang Thonglang). Meteorological stations: Survanabhumi and Don Mueang airport.

3. RESULTS AND DISCUSSION

This section discusses the key findings of the project period of March 2015 – October 2017, in which the sampling period was from September 2015 to February 2017.

3.1 Part 1: particulate matter monitoring results

3.1.1 PM Mass concentrations

Mass concentrations at both sites were analysed in both wet and dry period, separately, and the results for the whole sampling period from September 2015 – February 2017 and are presented in Figure 5. A summary of measurement results at both sites are presented in Table 4. The results showed higher PM levels during the dry period as compared to the wet period for both fine and coarse fractions at 2 sites. The high PM weeks were those having higher rain amount and vice versa (Figure 5).

The average concentrations of $PM_{2.5}$ and $PM_{>2.5}$ at PCD site in the wet period were $15 \pm 6 \mu\text{g}/\text{m}^3$ and $38 \pm 16 \mu\text{g}/\text{m}^3$, respectively, while in the dry period were $28 \pm 10 \mu\text{g}/\text{m}^3$ and $41 \pm 15 \mu\text{g}/\text{m}^3$, respectively. The highest $PM_{>2.5}$ concentration at PCD site was $83 \mu\text{g}/\text{m}^3$ obtained for the week 9 -16 November 2015, and the highest of $PM_{2.5}$ concentration was $50 \mu\text{g}/\text{m}^3$ obtained for the week 22 - 29 February 2016, both were in the dry period. The minimum level $PM_{2.5}$ and $PM_{>2.5}$ were found on 13-20 June 2016, i.e. the wet period, of $4 \mu\text{g}/\text{m}^3$, and $13 \mu\text{g}/\text{m}^3$, respectively. The monthly average of $PM_{2.5}$ ranged from 9 – 45 $\mu\text{g}/\text{m}^3$ while that of $PM_{>2.5}$ ranged from 21 – 72 $\mu\text{g}/\text{m}^3$. The highest monthly levels of $PM_{2.5}$ and $PM_{>2.5}$ were in February 2016 and November 2015 of 45 ± 5 and $72 \pm 8 \mu\text{g}/\text{m}^3$, respectively. Monthly levels of both fractions were the lowest in May 2016 (wet period), $9 \pm 3 \mu\text{g}/\text{m}^3$ and $21 \pm 7 \mu\text{g}/\text{m}^3$, respectively.

At AIT, the average $PM_{2.5}$ and $PM_{>2.5}$ in wet period were $15 \pm 5 \mu\text{g}/\text{m}^3$ and $37 \pm 16 \mu\text{g}/\text{m}^3$, respectively, as compared to the dry period of $32 \pm 11 \mu\text{g}/\text{m}^3$ and $44 \pm 18 \mu\text{g}/\text{m}^3$, respectively. The week of 13-20 February 2017 had the highest levels of $PM_{2.5}$ ($54 \mu\text{g}/\text{m}^3$) and the week of 9-16 November 2015 had the highest $PM_{>2.5}$ ($88 \mu\text{g}/\text{m}^3$). The lowest $PM_{2.5}$ level was $10 \mu\text{g}/\text{m}^3$ obtained for the week 13-20 June 2016, while that of $PM_{>2.5}$ was $12 \mu\text{g}/\text{m}^3$ obtained on 21-27 November 2016. Monthly average of $PM_{2.5}$ at AIT site ranged from 11-42 $\mu\text{g}/\text{m}^3$ while that of $PM_{>2.5}$ ranged from 18 – 73 $\mu\text{g}/\text{m}^3$. The highest monthly average of $PM_{2.5}$ was found in February of $41 \pm 17 \mu\text{g}/\text{m}^3$ while for $PM_{>2.5}$ was found in November 2015 of $73 \pm 11 \mu\text{g}/\text{m}^3$. The lowest monthly concentration of $PM_{2.5}$ was $11 \pm 1 \mu\text{g}/\text{m}^3$ recorded in June 2016 and $PM_{>2.5}$ of $18 \pm 4 \mu\text{g}/\text{m}^3$ recorded in November, 2016 due to some short-raining events.

To obtain a more coverage of the $PM_{2.5}$ monitoring data, the period average (September 2015 – February 2017) derived from hourly $PM_{2.5}$ data from available PCD stations (beta-ray method) was obtained as presented in Figure 6. The highest period average was seen at 54T which is located in the most polluted area in Bangkok (Din Daeng, roadside) of $36 \mu\text{g}/\text{m}^3$ which was well above the NAAQS of $25 \mu\text{g}/\text{m}^3$. In this study, the period average measured at AIT site was close to the NAAQS while in PCD site was measured slightly below the NAAQS. There were four stations where the period average concentrations were measured

well above the NAAQS (05T, 52T, 61T, and 27T) showing the high pollution levels of PM_{2.5} in the urban sites.

A comparison was specifically made for the monitoring results obtained from a PCD site (59T, the Government Public Relation Department) which is located not far away from the PCD building monitoring site (radius of <300 m) but measured at the different height. There is a positive correlation (R^2 0.499) between the data obtained from our measurement and those measured by the PCD site (59T) and the range of concentrations are comparable (Figure 7). However, our period average concentration (20.44 ± 11.5) was measured slightly lower than the PCD database (23.41 ± 8.1) showing that measurement at the ground may be directly affected by the major sources in the area.

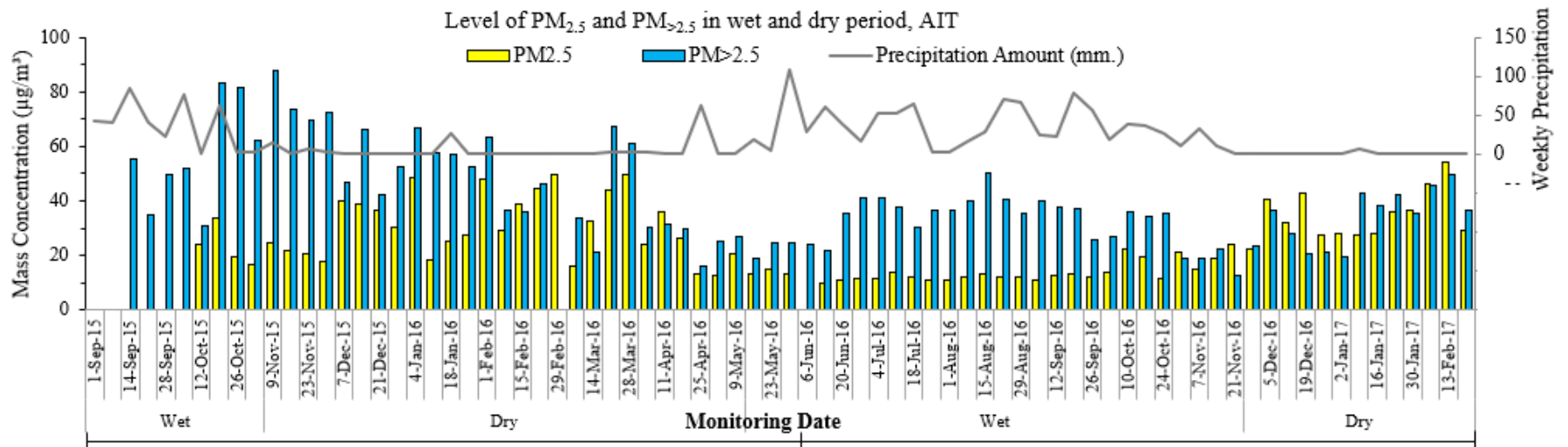
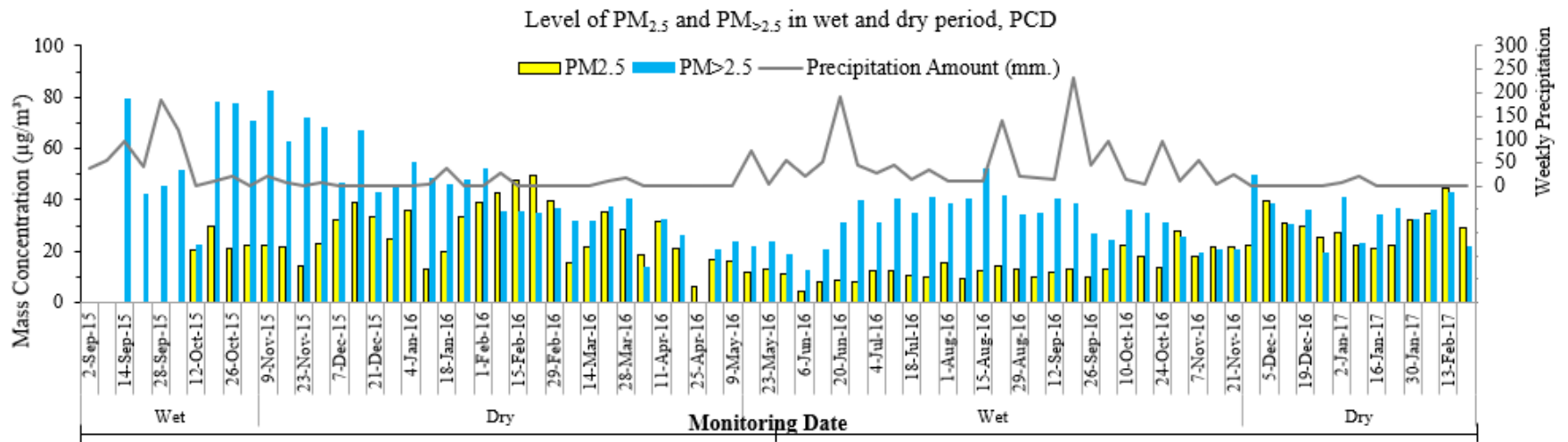


Figure 5 Mass concentrations of PM_{2.5} and PM_{>2.5} in wet and dry period at PCD and AIT site

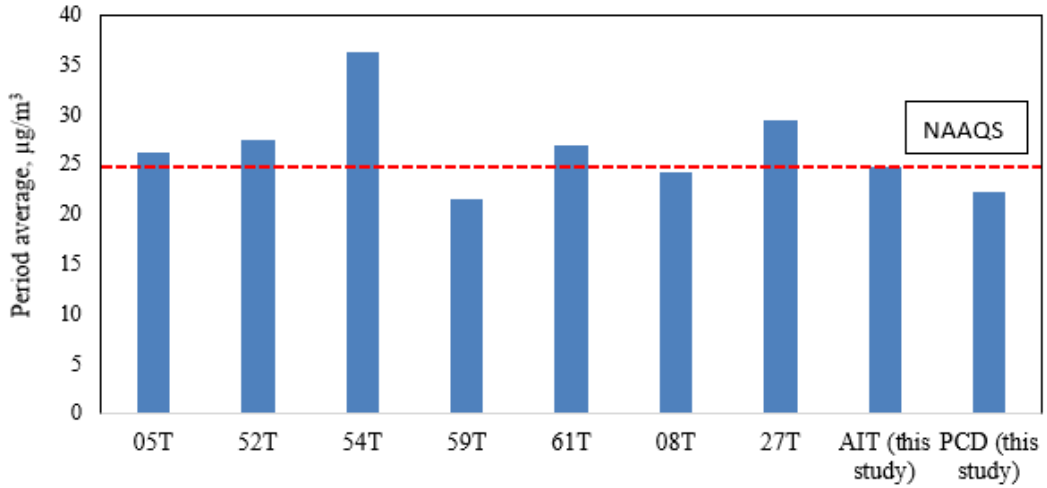


Figure 6 Period average of $\text{PM}_{2.5}$ (Sept 2015 – Feb 2017) calculated from the hourly-based monitoring results of PCD sites and weekly-based monitoring results conducted in this study (Note: refer to Figure 4 for the explanation and location of the sites)

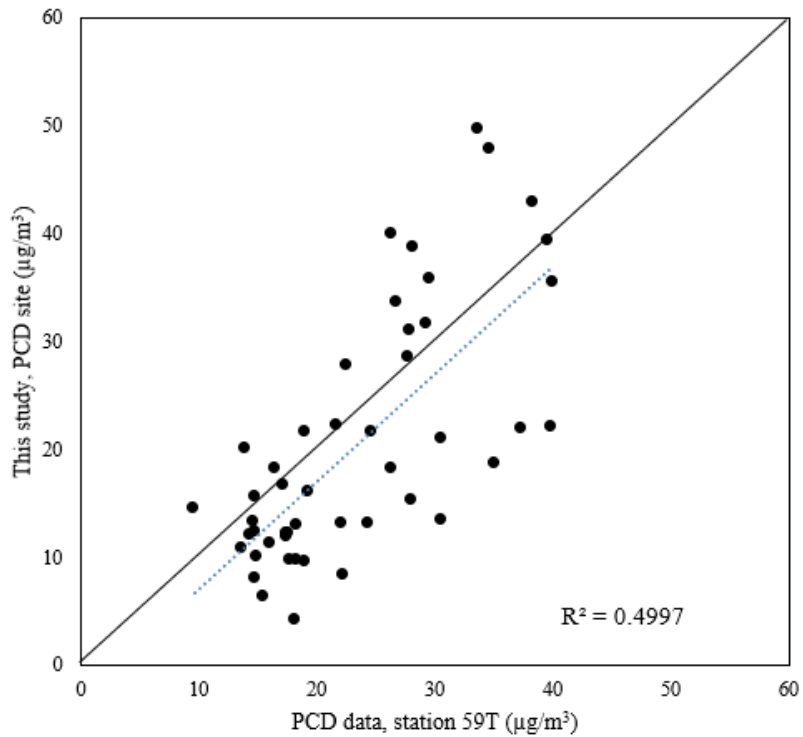


Figure 7 Comparison of weekly average concentrations at the PCD site measured in this study and the weekly average calculated from the hourly monitoring at station 59T (Note: refer to Figure 4 for the explanation and location of the sites)

3.1.2 Proportion of PM_{2.5} in SPM

The coarse fraction (PM_{>2.5}) is used for PM with diameter larger than 2.5 µm but it is not exactly the Total Suspended PM collected by a High-Vol sampler. The sum of mass of both size fractions is called the Suspended Particulate Matter (SPM). The ratio of PM_{2.5} to SPM shows the proportion of the fine PM in the SPM and it was 0.30 ± 0.10 and 0.42 ± 0.12 at PCD in the wet and dry period, respectively, while that of AIT was 0.31 ± 0.11 and 0.43 ± 0.11, respectively (Mahawong, 2017), as detailed in Table 4.

Table 4 Summary of Average Mass Concentration, SPM and PM_{2.5}/SPM ratio at AIT and PCD sites (in brackets are the ranges)

Site	Period	PM _{2.5} mass (µg/m ³)	PM _{>2.5} mass (µg/m ³)	SPM mass (µg/m ³)	PM _{2.5} /SPM (µg/m ³) ^a
PCD	Wet	14.6 ± 5.8 (4-28)	38 ± 17 (13-80)	50±19 (17-108)	0.30±0.10 (0.17-0.25)
	Dry	28 ± 10 (7-50)	41 ± 15 (14-83)	61±16 (32-106)	0.42±0.12 (0.17-0.59)
AIT	Wet	15.2 ± 5.3 (33-83)	37 ± 16 (12-83)	50±19 (32-117)	0.31±0.11 (0.19-0.44)
	Dry	32 ± 11 (13-54)	44 ± 18 (16-88)	75±23 (30-115)	0.43±0.11 (0.19-0.71)

Note: ^aaverage PM_{2.5}/SPM ratios were derived from the weekly PM_{2.5}/SPM data.

3.1.3 BC and EC/OC

BC concentrations in PM_{2.5} were measured using both PTFE filter (collected by the five-stage filter pack) and Quartz filter (collected by the two-stage filter pack) by OT21. The BC results were compared with EC and OC results produced by ACAP using the TOR method. Correlation of BC (IR) and EC for both filter types was made for each site. To take the advantage of OC data, this study used EC (and OC) results provided by ACAP for the source apportionment study.

A summary of the concentrations EC and OC at both sampling sites in wet and dry period is illustrated in Figure 6. The wet period had lower EC and OC (in PM_{2.5}) than the dry period at both sites, i.e. 2.25 ± 1.49 vs. 3.21 ± 1.23 and 2.36 ± 2.26 vs. 6.12 ± 3.02 µg/m³, respectively at PCD while at AIT i.e. 2.45 ± 0.91 vs. 4.14 ± 1.22 and 2.50 ± 1.88 vs. 8.54 ± 2.94 µg/m³, respectively. Similar conditions were also found for the EC and OC measured in PM_{>2.5} as presented in Figure 6. Overall, the average EC and OC concentrations in PM_{2.5} were measured respectively higher at AIT of 3.60 ± 2.19 µg/m³ and 5.52 ± 4.59 µg/m³ than at PCD of 2.75 ± 1.44 µg/m³ and 4.29 ± 3.34 µg/m³. The levels of EC and OC were lower in the coarse PM, i.e. EC and OC in PM_{>2.5} were 0.84 ± 0.55 µg/m³ and 1.80 ± 0.67 µg/m³, respectively, at PCD while the corresponding levels at AIT were 1.07 ± 0.57 µg/m³ and 2.40 ± 1.97 µg/m³.

Ratio of EC to total carbon (TC=EC+OC) was calculated to indicate the both sources of combustion and also the potential of wet removal as presented in Appendix 3. The ratio of EC to TC in PM_{2.5} at PCD site in dry period was approximately 0.34, while in wet period was 0.37.

Previous studies in the BMR region (Kim Oanh et al., 2010a, 2010b) have reported higher BC/TC ratio of ~ 0.7 from diesel emission and lower values of ~ 0.15 near the rice straw open burning sources. During the dry season when traffic and rice straw open burning emissions are intensive, the ambient BC/TC ratio is lower as compared to the wet season when it has less open burning emission and higher contribution of traffic emission (i.e. diesel vehicle) to the total emission. Previous source apportionment study in BMR also found that contribution of the traffic emission was more dominant in the wet season (40.7%) than in dry season (29.5%) (Kim Oanh et al., 2013). Note that, in the wet season part of water-soluble organic carbon (WSOC) can be washed out that changes the EC/TC ratio for PM. Therefore, in future studies the WSOC in rain water (wet deposition) should also be considered.

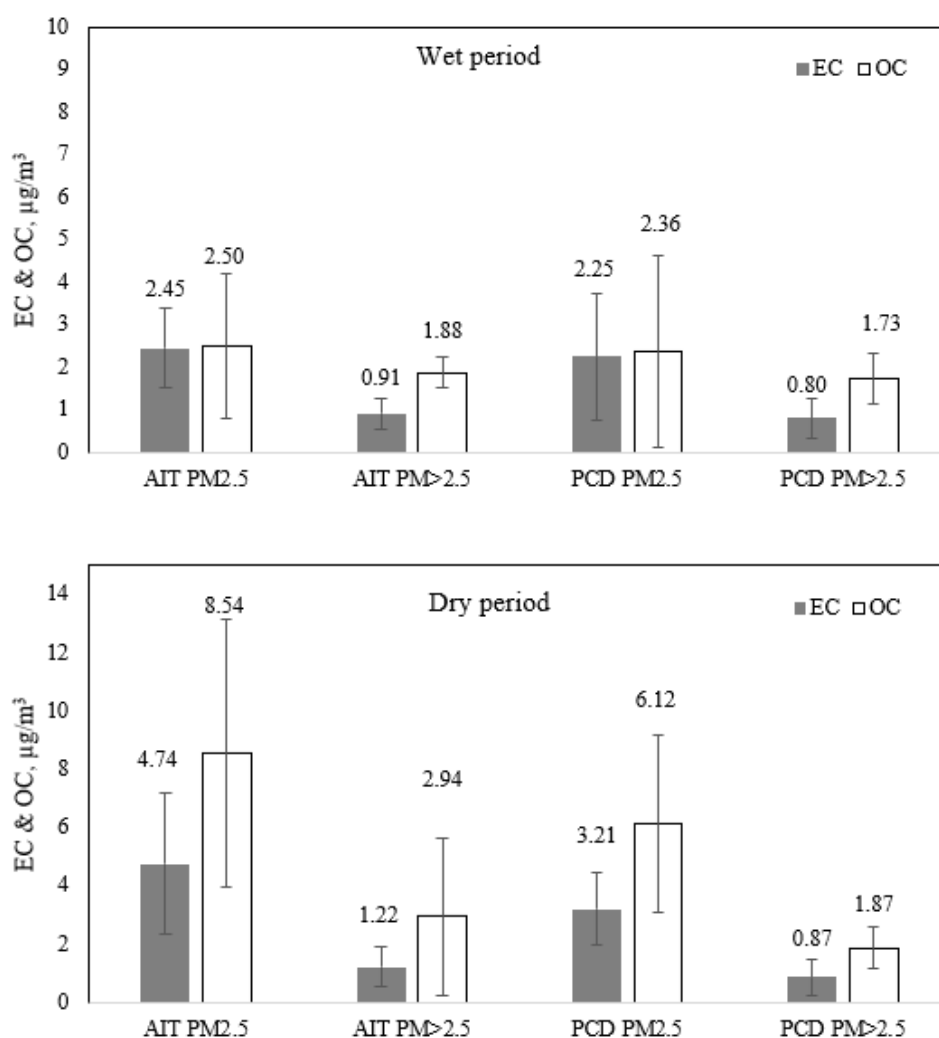


Figure 6 EC and OC in PM_{2.5} and PM_{>2.5} at AIT and PCD sites in wet and dry period

3.1.4 Ion concentration

The ionic levels at PCD in the wet and dry periods are shown in Figure 7 that showed the most dominant anion in PM_{2.5} being sulfate contributing $2.49 \mu\text{g}/\text{m}^3$ in wet and $3.22 \mu\text{g}/\text{m}^3$ in dry period. Ammonium ion contributed the most of cations in both periods, i.e. $0.79 \mu\text{g}/\text{m}^3$ in wet and $1.41 \mu\text{g}/\text{m}^3$ in dry period. In PM_{>2.5}, nitrate had the largest level among

anions in both periods, $1.33 \mu\text{g}/\text{m}^3$ in wet and $3.08 \mu\text{g}/\text{m}^3$ in dry period, while calcium was the most dominant cation, $1.00 \mu\text{g}/\text{m}^3$ in wet period and $1.66 \mu\text{g}/\text{m}^3$ in dry period.

Figure 8 presents the ionic composition of PM at AIT site for both periods that show a quite similar picture of those obtained at PCD. In $\text{PM}_{2.5}$, the most dominant anion was also sulfate which contributed of $2.37 \mu\text{g}/\text{m}^3$ in wet and $4.10 \mu\text{g}/\text{m}^3$ in dry period. Ammonium ion contributed the highest among the cations in both periods. For $\text{PM}_{>2.5}$, nitrate ion had the largest anion concentration, $1.14 \mu\text{g}/\text{m}^3$ in wet and $2.71 \mu\text{g}/\text{m}^3$ in dry period while calcium was the most dominant among cations, $1.10 \mu\text{g}/\text{m}^3$ in wet period and $2.1 \mu\text{g}/\text{m}^3$ in dry period.

On average, higher levels of sulfate, nitrate and ammonium were found in $\text{PM}_{2.5}$ in dry than wet period at both sites indicating an efficient wet removal of the components. Higher levels of potassium in the dry than wet period at both side also indicated more contribution of biomass burning smoke. In the coarse PM, high levels of calcium indicated for example the contribution from soil dust and/or construction activities and higher level of this ion in the dry period would indicate more intensive contribution from these sources in the dry period.

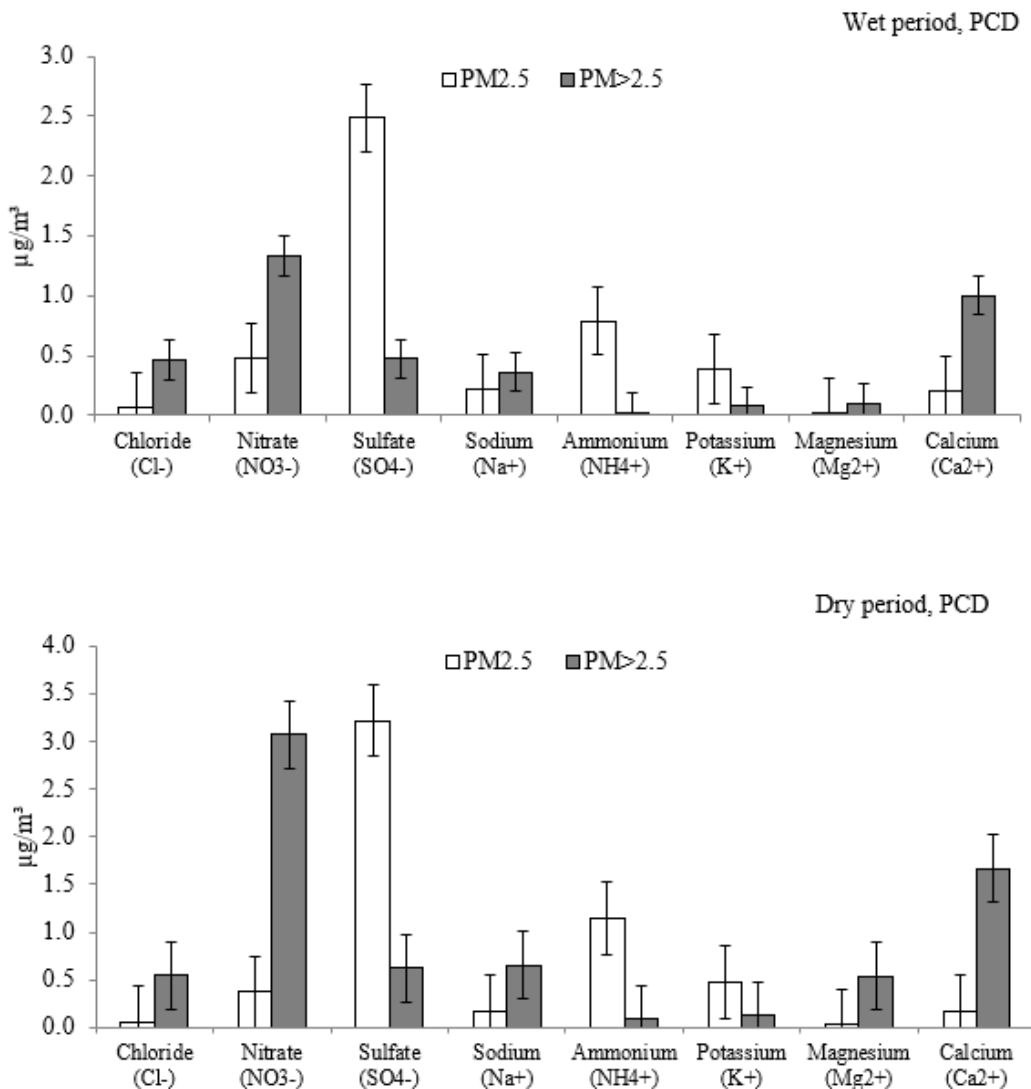


Figure 7 Levels of ions in PM_{2.5} and PM_{>2.5} in wet and dry period at PCD site

The ion balance (between sum of cations and sum of anions in equivalents) for PM_{2.5} collected at both sites, in wet and dry period, is presented in Appendix 4. The linear regression lines between cations and anions had high R² of >0.90 at both sites except for the AIT site during the dry period that had lower R² (0.77). The slopes of all lines were 1.18-1.30 which showed more abundance of basic components as compared to acidic ones. Lower the slopes obtained during the wet season further suggested a more efficient wet removal of the acidic components. A lower R² obtained for the AIT site during the dry period was mainly caused by a local source of NH₃, e.g. from the ongoing sanitation experiments in the AIT ambient lab. The regression lines between the sum of cations and the sum of anions for coarse fraction had lower R², especially for the AIT site. The coarse fraction may contain other components that were not analysed in this project. Overall, organic ions as well as CaCO₃ and HCO₃⁻ were not analysed in this study which may be a reason for the imbalance of the ions in PM (the slope of regression line differed from 1.0). Higher concentrations of Cl⁻, NO₃⁻, Na⁺, Mg²⁺, Ca²⁺ were found in coarse PM than fine PM, while on the contrary the higher concentrations of SO₄²⁻, NH₄⁺, and K⁺ were found in the fine PM than in coarse PM in both of wet and dry period at AIT and PCD site (see Figure 7 and Figure 8).

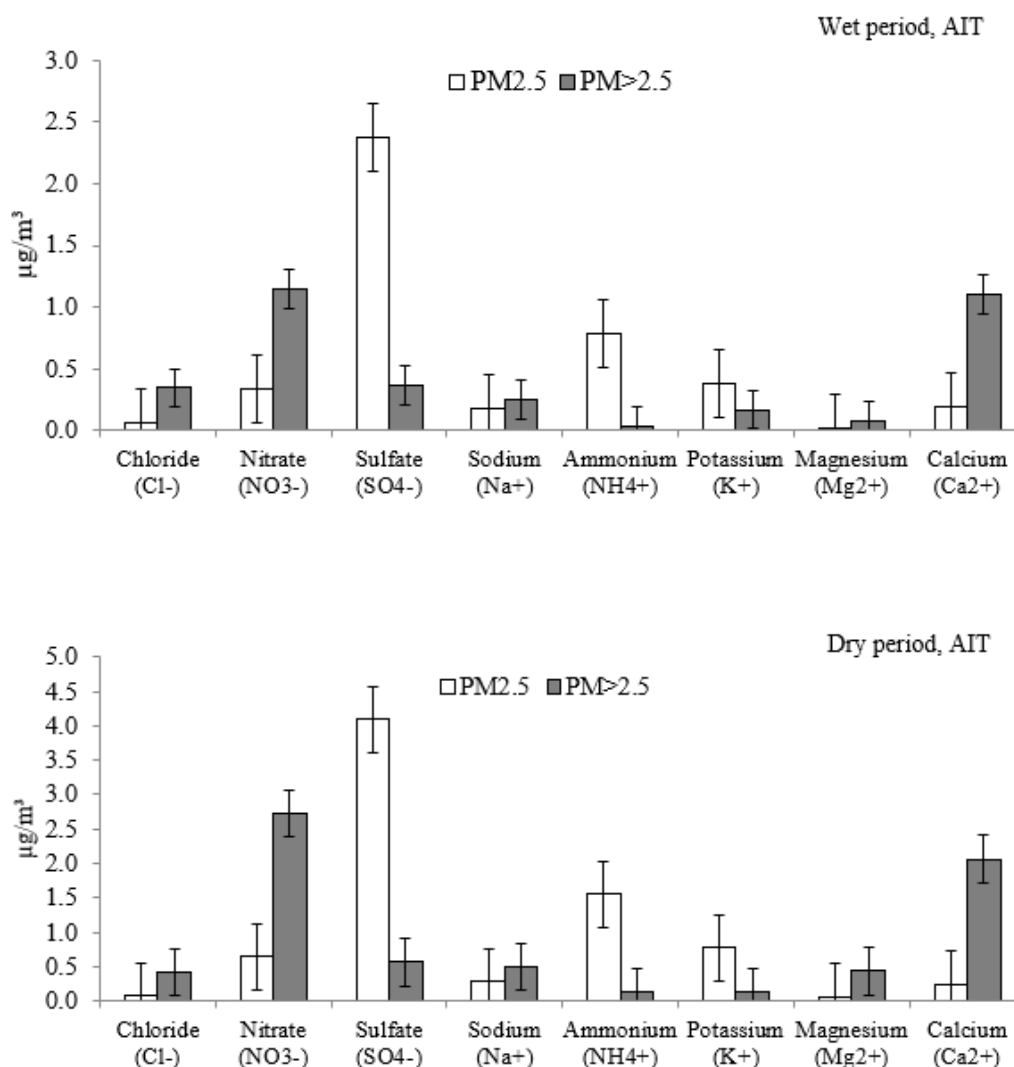


Figure 8 Levels of ions in PM_{2.5} and PM_{>2.5} in wet and dry period AIT site

3.1.5 Element concentration

The quartz filter samples of PM_{2.5} and PM_{>2.5} from 2-stage filter packs were analysed at ACAP for 40 elements (Li, Be, Na, Mg, Al, K, Ca, Sc, V, Cr, ⁵⁴Fe, ⁵⁶Fe, Mn, Co, Ni, Cu, Zn, Ga, As, Ar, Se, Kr, Rb, Sr, Y, Mo, Ag, Cd, In, Sb, Cs, Ba, Hg, Tl, ²⁰⁶Pb, ²⁰⁷Pb, ²⁰⁸Pb, Bi, Th and U) and the data is used in this research. One quarter of a filter was extracted into 15 mL for the analysis. The element composition can serve as useful markers of contributing sources to the PM measured at the sites. For example, marker elements of diesel vehicle exhaust could be Cu, Fe and Zn. The elements were therefore added in this project although originally not planned. The initial results were available but still need more analysis to be presented hence once ready they will be presented in our journal papers.

3.1.5 Source apportionment using receptor modeling

a) Reconstructed mass

The reconstructed mass (RCM) was done using the mass groups similar to those presented in Kim Oanh et al. (2016) to provide information on major contributing sources. The percentage of mass explain of some samples were excluded from the RCM calculation because the exceedance of 100% which was mainly due to low levels in low PM mass hence having high analytical uncertainty. The reconstructed mass results are presented in Figure 9. The largest component in PM_{2.5} were organic matter (OM)-biomass in dry period at both sites which accounted for 5.96 µg/m³ in PCD and 9.87 µg/m³ in AIT suggesting the contribution from biomass burning sources. The major components in PM_{>2.5} were NO₃⁻ and Ca²⁺ at both sites indicated the contribution of aged sea salt and the soil/road dust. Note that the preliminary results of elements were also included in this RCM calculation. There were high percentages of unexplained mass for coarse PM in both sites which suggested the inclusion of carbonate and other crustal elements may be necessary for a better mass closure. For the fine fraction the mass closure was much better with a small percentage of unexplained mass.

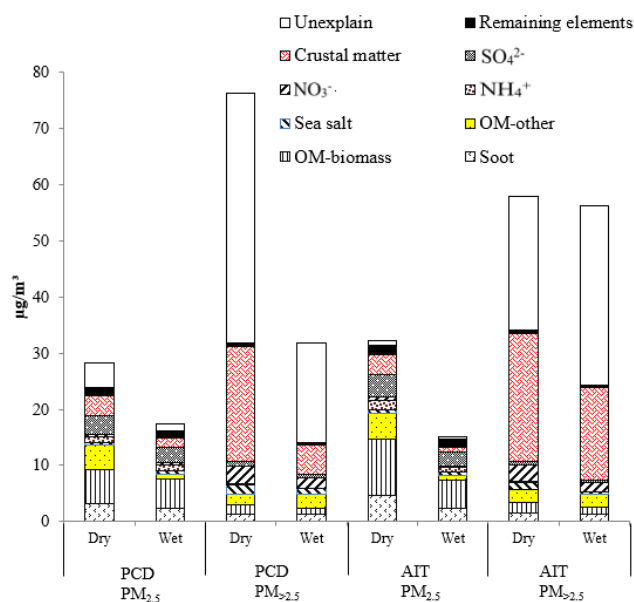


Figure 9 Reconstructed mass for PM_{2.5} and PM_{>2.5} at PCD and AIT in the dry and wet period

b) Source apportionment by CMB

CMB was run for weekly samples and the average results are presented in Figure 10 for PM_{2.5} in the dry and wet period. At PCD site, the highest contribution to PM_{2.5} in wet period was diesel vehicles (28%), biomass burning (26%) and inorganic secondary PM (21%). In the dry period, the biomass burning had the highest contribution (35%), followed by diesel vehicles (21%), inorganic secondary PM (15%) and industrial emission (3.4%). At AIT site, the highest contribution to PM_{2.5} in wet period was diesel vehicles (29%), biomass burning (25%) and inorganic secondary PM (20%). In the dry period the biomass burning had the highest contribution (38%), followed by diesel vehicles (27%), inorganic secondary PM (15%) and industrial emissions (5%). There were other sources which had minor contributions to PM_{2.5} including soil, sea salt, aged sea salt, and oil burning. Note that the secondary particles are formed in the atmosphere hence the precursor sources (i.e. SO₂ sources), both local and regional, need to be further investigated.

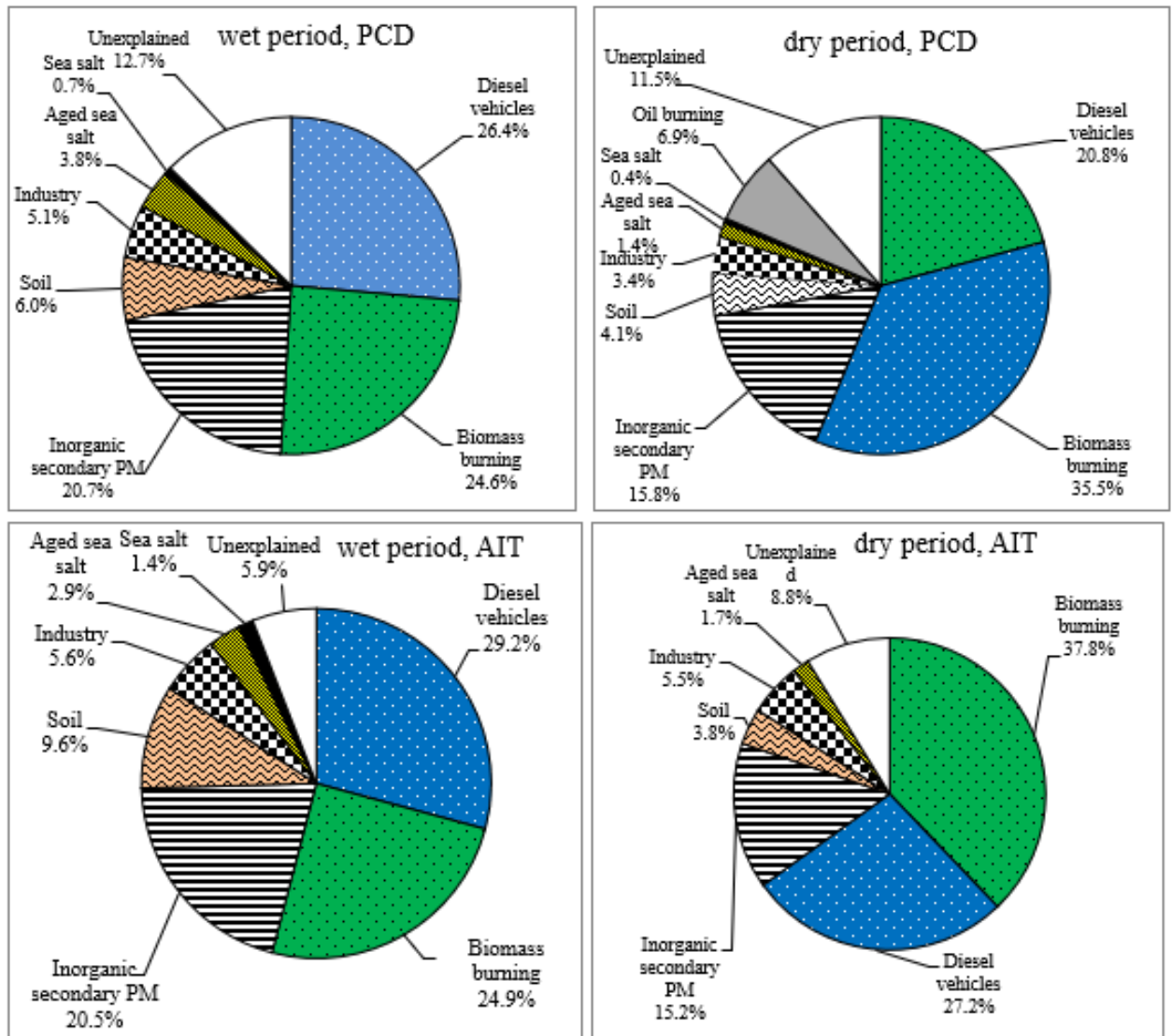


Figure 10 Average source contributions to PM_{2.5} in wet and dry periods at AIT and PCD

Note: Inorganic secondary PM: secondary sulfate + secondary nitrate, industrial emission: lead + steel + zinc, and aged sea salt: NaNO₃

c) Preliminary source apportionment results by PMF

PMF produced the contributions for each source sector in every weekly PM_{2.5} sample. The average results for the wet period and dry period, respectively, were obtained for the source analysis. Due to the lack of final element data, only preliminary results of PMF could be produced and that for PCD site in the wet period are presented in Appendix 5 as an example. For PM_{2.5} in wet period at PCD site, secondary PM (24%) was the most dominant source factor, followed by soil/road dust (23%), diesel vehicles (21%), industrial (20%), biomass burning (12%), and.

Note that, PMF results at could not foster the explainable source profiles due to the uncertainty in the element data. Therefore, AIT and ACAP further scrutinize and double check the element data which will be included in the journal publication as well as the policy brief of the project.

3.1.6 Trajectory analysis

The results of HYSPLIT back trajectory showed the travelling path of air mass before it reached the sampling sites. The weekly samples were chosen to include the highest PM_{2.5} mass week and the lowest mass week at each site. In general, the wet season has the prevalent southwest monsoon while the dry season is dominated by northeast monsoon. Less rain and more stagnant air (in addition to more open burning) in the dry season as compared to the wet season that contribute to high PM levels in the dry season. Five (5) days backward HYSPLIT trajectories for the selected weeks were obtained at PCD and AIT sites and the results are presented in Appendix 6.

At PCD site, during the period of 13-20 February 2017 when PM concentration was high, the airmass mainly arrived from the Continental Southeast Asia (regional pathway). Whereas, during the period of 3-10 October 2016, low PM week, the airmass originated from the sea, i.e. in the Gulf of Thailand, with a long marine pathway hence was not expected to bring in significant long-range transport emission to the site. A similar pattern was seen for the AIT site, during the period of 13-20 February 2017, the airmass originated from the continent hence the PM was measured high. During the period of 24-31 October 2016, the airmass had a long marine pathway from the Andaman Sea and the PM concentrations were measured low. The HYSPLIT backward trajectories provided some insight into the upwind source regions and potential long-range transport pollution to the measured PM at the sites. However, there are other interrelated factors affecting the PM levels, e.g. the marine pathways (SW monsoon) would induce rain that enhance the wet removal and limit the open burning emission. On the opposite, the continental pathways associated with the NE monsoon would induce dry weather, stagnant atmosphere, and more open burning emission.

3.2 Part 2: acid deposition

This section presents the key results of the acid deposition monitoring, such as pH of rain water, electrical conductivity, ion concentration of rain water, deposition velocity and deposition fluxes.

3.2.1 pH of rainwater

The observed that the average of pH values measured at PCD and AIT sites are presented in Figure 11. The range of pH was 4.59 – 7.16 at PCD and 4.69-7.03 at AIT. The minimum value at both sites occurred in April, 2015. In wet period, the average pH at PCD and AIT sites was 5.59 ± 0.73 and 5.77 ± 0.62 , respectively. In the dry period, the average pH value at PCD and AIT was 4.91 ± 0.82 and 5.18 ± 0.79 , respectively. The percentage of acid rain results, i.e. $\text{pH} \leq 5.6$, at PCD and AIT sites was 40% and 20% respectively.

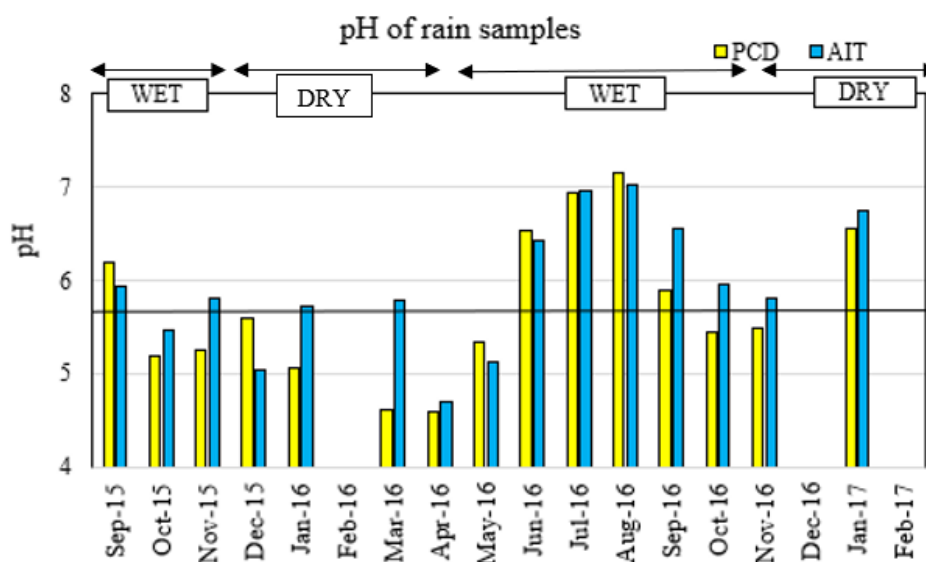


Figure 11. pH variations at PCD and AIT sites

3.2.2 Electrical conductivity

The average (and range) of electrical conductivity (EC) measured at PCD and AIT sites were 2.02 ± 1.11 (0.95 – 4.89) and 2.08 ± 1.65 mS/m (0.88 – 7.52 mS/m), respectively. In the wet period, the average conductivity at PCD and AIT sites was 1.44 ± 0.44 and 1.52 ± 0.50 , lower than those measured in the dry period of 3.40 ± 1.09 and 3.38 ± 2.81 mS/m, respectively. The highest values were measured at both sites in March 2016 and this may be due to low precipitation in this dry period. The EC levels represent the amount of total dissolve solid hence lower precipitation induces higher concentrations of chemical species hence higher EC. This also means that the rain has dissolved various ionic species in the air that were deposited in the wet deposition flux to the earth surface. The monthly levels of electrical conductivity are shown in Figure 12.

3.2.2 Monthly weighted average ionic concentrations in rainwater

The ionic concentration in the rain water, in $\mu\text{eq/L}$, collected at the PCD site was found in the rank of $\text{NH}_4^+ > \text{Ca}_2^+ > \text{NO}_3^- > \text{SO}_4^{2-} > \text{Cl}^- > \text{Na}^+ > \text{Mg}^{2+} > \text{K}^+$. A similar rank was found for ionic species at AIT but with only a switch of the first 2 major cations, i.e. $\text{Ca}_2^+ > \text{NH}_4^+ > \text{NO}_3^- > \text{SO}_4^{2-} > \text{Cl}^- > \text{Na}^+ > \text{Mg}^{2+} > \text{K}^+$, as shown in Figure 13. The major anion was NO_3^- which was 38.3 ± 22.9 and 60.6 ± 53.5 $\mu\text{eq/L}$ at PCD and AIT, respectively. The major cation at PCD site was NH_4^+ of 64.3 ± 25.0 $\mu\text{eq/L}$ while the major of cation at AIT site was Ca^{2+} of 92.5 ± 77.7 $\mu\text{eq/L}$. The trend of the monthly weighted average ionic concentrations in rainwater showed that ionic concentrations decreased during wet period while in the dry period, the ionic concentration increased because of the high concentration in relatively small amount of the precipitation (Appendix 7). Note that the weighted average monthly concentrations are related to the results of electrical conductivity presented above.

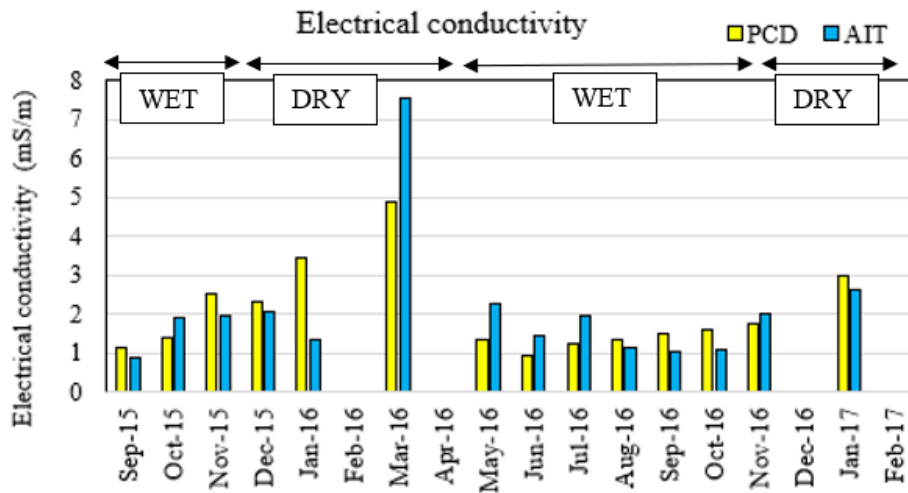


Figure 12. Variation of electrical conductivity of rain samples at PCD and AIT sites

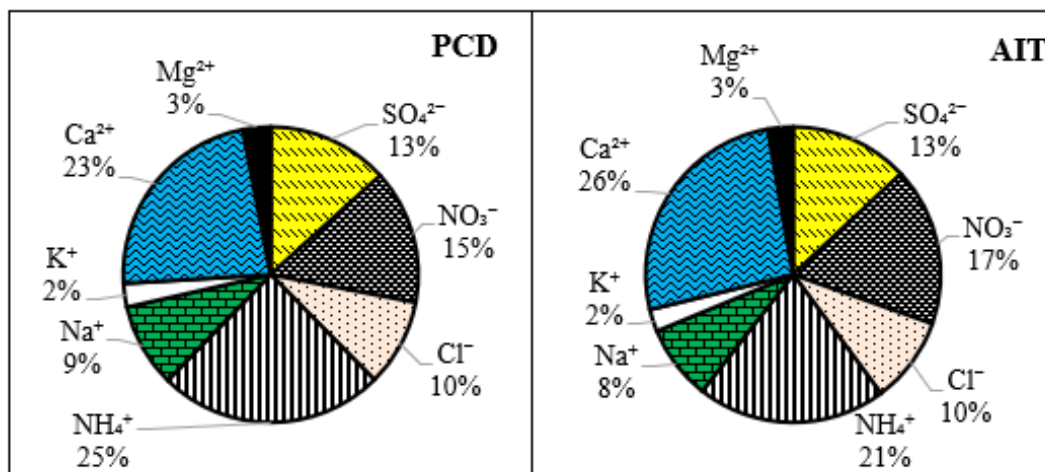


Figure 13. Share of ionic species to the total measured ions amount

3.2.3 Wet deposition flux

The total wet deposition fluxes of the species at both sites followed the same rank of $\text{NH}_4^+ > \text{Ca}_2^+ > \text{NO}_3^- > \text{SO}_4^{2-} > \text{Cl}^- > \text{Na}^+ > \text{K}^+ > \text{Mg}^{2+}$ (Figure 14). In the wet period, the high precipitation amount at both sites induced high wet deposition fluxes than in the dry period. It was observed that the main ion species in the wet deposition were NH_4^+ , Ca^{2+} , NO_3^- , and SO_4^{2-} .

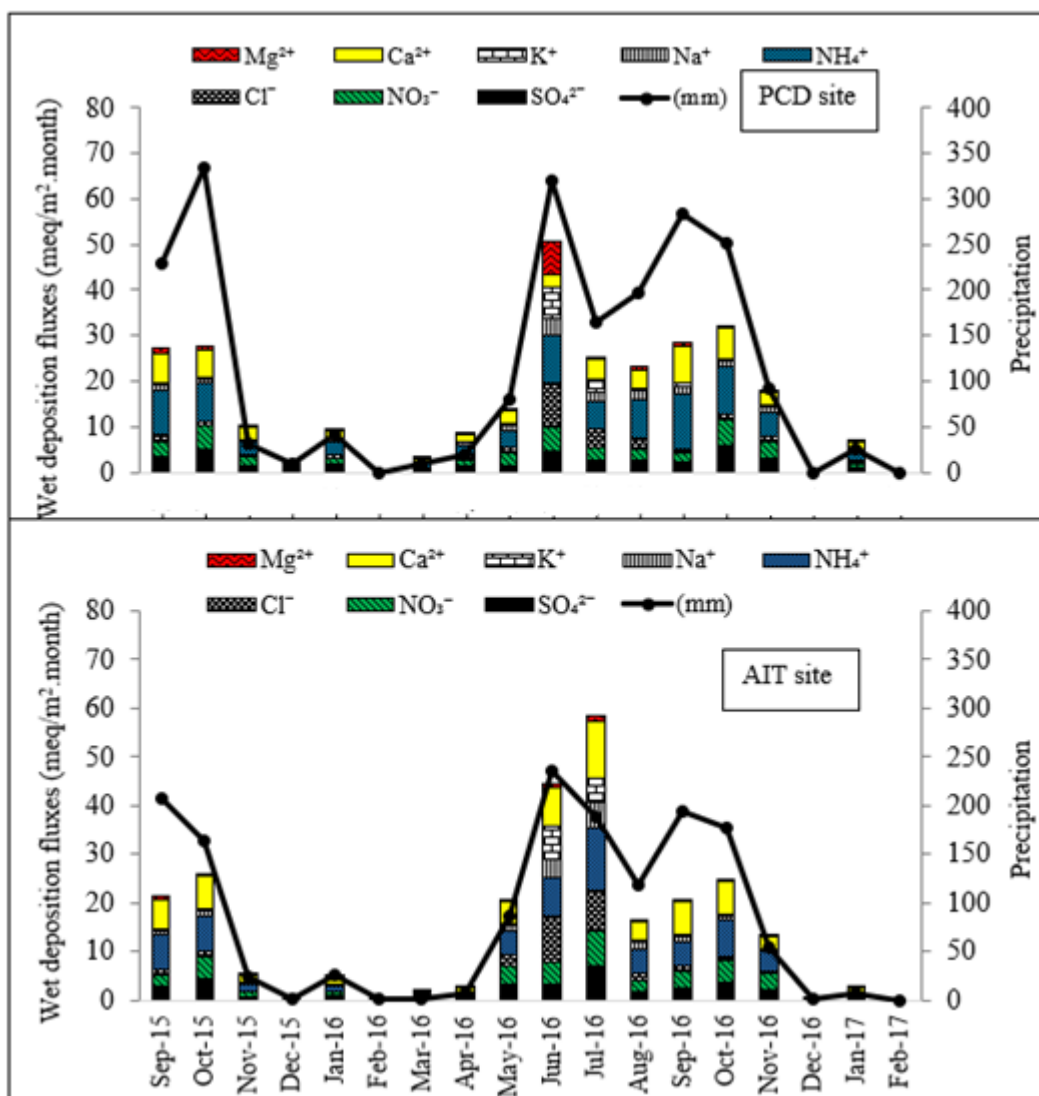


Figure 14. Monthly wet deposition fluxes at PCD and AIT sites

3.2.4 Atmospheric concentration of gaseous pollutants

The gaseous pollutants were collected using F1, F2 and F3 stages of the filter pack. Table 5 gives a summary of the gaseous concentration results. The gas concentrations at both sites were ranked as follow: $\text{NH}_3 > \text{SO}_2 > \text{HNO}_3 > \text{HCl}$. The average concentrations over the entire monitoring period of the gaseous pollutants measured at AIT were generally slightly lower than those measured at PCD but overall the levels at both sites are comparable. Exception was for NH_3 which was slightly higher at AIT than PCD although the ranges were largely overlapped. The high NH_3 levels collected at AIT during the months of January 2016-July 2016 may be due to the influence of the sanitation experiments at the ambient lab as well as other agricultural activities in the AIT site surrounded by more rural set-up as compared to PCD.

Table 5. Monthly Average Gaseous Concentration (ppb) at PCD and AIT Sites

Site	Month	Weighted monthly concentration (ppb)			
		SO ₂	HNO ₃	HCl	NH ₃
PCD	Sep-15	1.6	0.3	0.3	10.1
	Oct-15	2.2	1.3	0.4	11.7
	Nov-15	2.6	1.4	0.6	17.1
	Dec-15	3.0	2.0	0.8	16.1
	Jan-16	2.7	1.8	0.8	13.0
	Feb-16	0.6	1.8	1.0	12.2
	Mar-16	2.6	1.1	1.0	11.6
	Apr-16	1.4	0.8	0.9	10.5
	May-16	0.4	0.5	0.4	10.4
	Jun-16	1.1	0.2	0.4	11.4
	Jul-16	2.4	0.4	0.4	14.6
	Aug-16	1.8	0.3	0.7	14.8
	Sep-16	2.3	0.3	0.5	14.9
	Oct-16	2.1	0.9	0.5	14.7
	Nov-16	2.2	1.3	0.6	17.3
	Dec-16	2.7	1.4	0.7	16.2
	Jan-17	2.9	1.3	0.8	17.8
	Feb-17	2.3	1.7	1.0	8.4
Average		2.1 ± 0.75	1.0 ± 0.60	0.7 ± 0.23	13.5 ± 2.84
AIT	Sep-15	1.2	0.4	0.4	10.2
	Oct-15	0.9	0.6	0.3	10.8
	Nov-15	1.8	0.9	0.4	15.3
	Dec-15	2.0	1.1	0.6	14.8
	Jan-16	0.4	1.7	0.7	17.0
	Feb-16	0.5	2.0	0.9	17.6
	Mar-16	2.3	1.6	0.9	19.6
	Apr-16	0.9	1.1	1.2	16.5
	May-16	0.3	1.0	0.7	15.0
	Jun-16	0.9	0.3	0.3	16.3
	Jul-16	1.5	0.4	0.3	15.1
	Aug-16	1.4	0.2	0.6	15.6
	Sep-16	1.0	0.3	0.4	13.8
	Oct-16	2.0	0.6	0.4	13.5
	Nov-16	2.0	0.9	0.5	16.0
	Dec-16	2.0	1.1	0.6	14.8
	Jan-17	2.2	1.1	0.8	18.4
	Feb-17	1.8	1.8	1.0	9.3
Average		1.4 ± 0.64	0.9 ± 0.54	0.6 ± 0.26	15 2.73

3.2.5 Deposition velocity of gases

Dry deposition velocity of each gas species was estimated by the resistance model provided in EXCEL template of the resistance model provided by ACAP (2017) for both gases and PM. The results are summarized in Table 6.

In order to calculate the dry deposition velocity of the ionic components in PM, first the monthly average concentrations of ionic components of PM were calculated and the results are presented in Appendix 8. The average concentrations of the selected 3 ionic species in PM were slightly higher at AIT than PCD. At both sites higher levels were seen during the dry period than the wet period.

Table 6 Average Dry Deposition Velocity over Different Surface Types for PCD and AIT from September 2015- February 2017

Species	Vd (cm/s) over the surface				
	Water	Tree	Building & Road	Grass	Agricultural
PCD site					
SO ₂	0.23±0.22	0.83±0.62	0.17±0.01	0.57±0.37	0.46±0.31
HNO ₃	0.22±0.22	3.11±2.67	3.25±3.2	1.10±0.97	0.97±0.93
NH ₃	0.24±0.04	0.25±0.13	0.05±0.001	0.23±0.1	0.30±0.16
pSO ₄ ²⁻	0.05±0.04	0.46±0.5	0.06±0.03	0.12±0.06	0.08±0.05
pNO ₃ ⁻	0.05±0.04	0.55±0.58	0.06±0.04	0.12±0.06	0.08±0.05
pNH ₄ ⁺	0.05±0.04	0.44±0.46	0.06±0.05	0.12±0.06	0.08±0.05
AIT site					
SO ₂	0.27±0.09	1.15±0.52	0.25±0.26	0.77±0.17	0.60±0.17
HNO ₃	0.27±0.09	4.33±0.90	4.22±1.56	1.52±0.33	1.24±0.43
NH ₃	0.29±0.10	0.32±0.14	0.08±0.11	0.28±0.08	0.43±0.1
pSO ₄ ²⁻	0.10±0.02	0.64±0.18	0.09±0.04	0.12±0.02	0.15±0.03
pNO ₃ ⁻	0.10±0.02	0.80±0.22	0.09±0.05	0.12±0.02	0.15±0.04
pNH ₄ ⁺	0.10±0.02	0.63±0.17	0.09±0.06	0.12±0.02	0.15±0.05

The highest deposition velocity of SO₂ was seen over the tree cover, while for NH₃ it was high over the agricultural land. For HNO₃, the deposition velocity was high above both tree and building cover. The highest monthly average SO₂ dry deposition velocity at PCD and AIT sites were found in September, 2015, i.e. 2.05 and 2.00 cm/s, respectively. For HNO₃ it was found in January 2016 (8.9 cm/s) at PCD and April 2016 (6.9 cm/s) at AIT. The highest monthly average dry deposition velocity of NH₃ at PCD site was found in December, 2015 (0.65 cm/s) while at AIT it was found in September, 2016 (0.58 cm/s).

3.2.6 Dry deposition fluxes

The dry deposition fluxes were calculated from the monthly average deposition velocity (Table 6) by multiplying with air concentrations measured in the respective month. The results of time varying dry deposition fluxes of sulfur and nitrogen discussed separately

below. Monthly average deposition velocity calculated using the resistance model provided by ACAP is presented in Appendix 10.

a. Sulfur deposition

The monthly average dry deposition amount of sulfur compounds (gases and PM) from September 2015 - February 2017 were 0.44 ± 0.24 at PCD and 0.59 ± 0.27 mmol/m².month at AIT. The maximum dry deposition flux of sulfur compounds at PCD occurred in December, 2015 of 0.97 mmol/m².month and at AIT in March 2016 of 1.17 mmol/m².month as seen in Figure 15.

b. Nitrogen deposition

The monthly average dry deposition amount of nitrogen compounds (gases and PM) from September 2015 - February 2017 at PCD and AIT site were 5.32 ± 5.80 and 6.72 ± 2.22 mmol/m².month, respectively. The maximum dry deposition flux of nitrogen compounds at PCD site occurred in December, 2015 (18.38 mmol/m².month) while at AIT site it occurred in March, 2016 (11.69 mmol/m².month) as seen in Figure 16.

3.2.7 Total deposition amount

The total deposition amount was estimated by the sum of dry deposition and wet deposition fluxes. Higher total deposition amounts of sulfur and nitrogen compounds were observed in the wet period. The wet deposition was dominant during the wet period which showed that wet deposition played an important role to remove sulfur and nitrogen species from the atmosphere. The total deposition of sulfur compounds during September 2015 – February 2016 (over 18 months) at PCD and AIT sites were 837 and 821 kg/km², respectively, while the total nitrogen compounds were 3,132 and 3,043 kg/km², respectively.

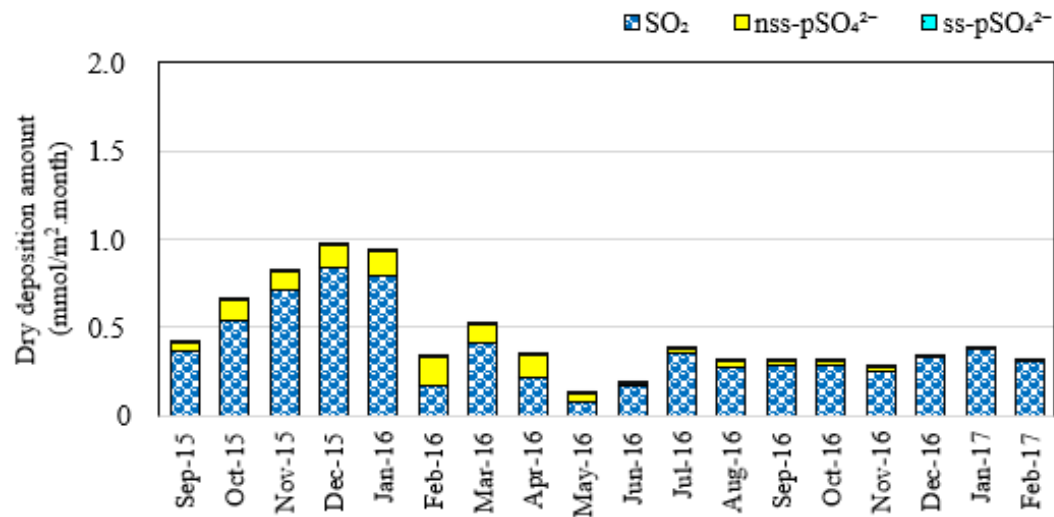
The critical load of sulfur in Thailand was adapted by Milindalekha, (2001) and the value was considered as a threshold. The sulfur deposition in 2016 was 586 kg/km².yr that was lower than the critical load (3,000 – 5,000 kg/km².yr). Likewise, the nitrogen deposition flux was 2,235 kg/km².yr that was also lower than the critical load (6,090 - 9,030 kg/km².yr) as presented in Table 7. Thus, in 2016 the total annual deposition of sulfur and nitrogen compounds were estimated to be lower than the critical load values, meaning that the environment in Pathumthani province still has buffering capacity to neutralize the acid deposition. However, the situation may be getting worse if the emissions are not controlled in the near future.

Table 7. Current Sulfur and Nitrogen deposition in Pathumthani Province compared to the critical load values

Parameters	S deposition (kg/km ² .yr)	N deposition (kg/km ² .yr)
Actual sulfur deposition	586	2,235
Critical load approach	3,000 – 5,000*	6,090 – 9,030**
Potential risk	No	No

* Critical load values of sulfur for Pathumthani province from Milindalekha, 2011.

** Critical load values of nitrogen adapted for Pathumthani province from Bouwman & Van Vuuren (1999)



Dry deposition amount of sulfur compounds at AIT

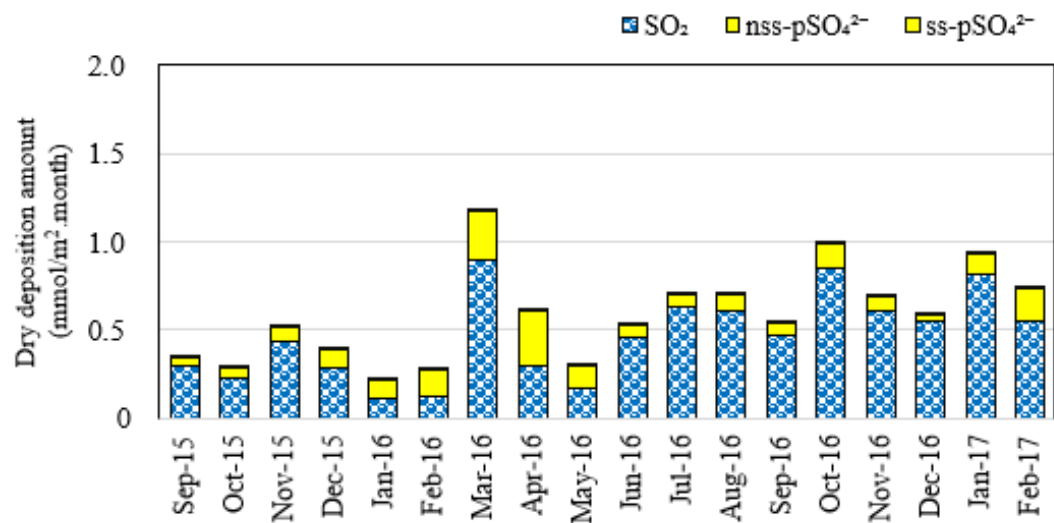


Figure 15. Monthly average dry deposition fluxes of sulfur compounds at PCD and AIT site

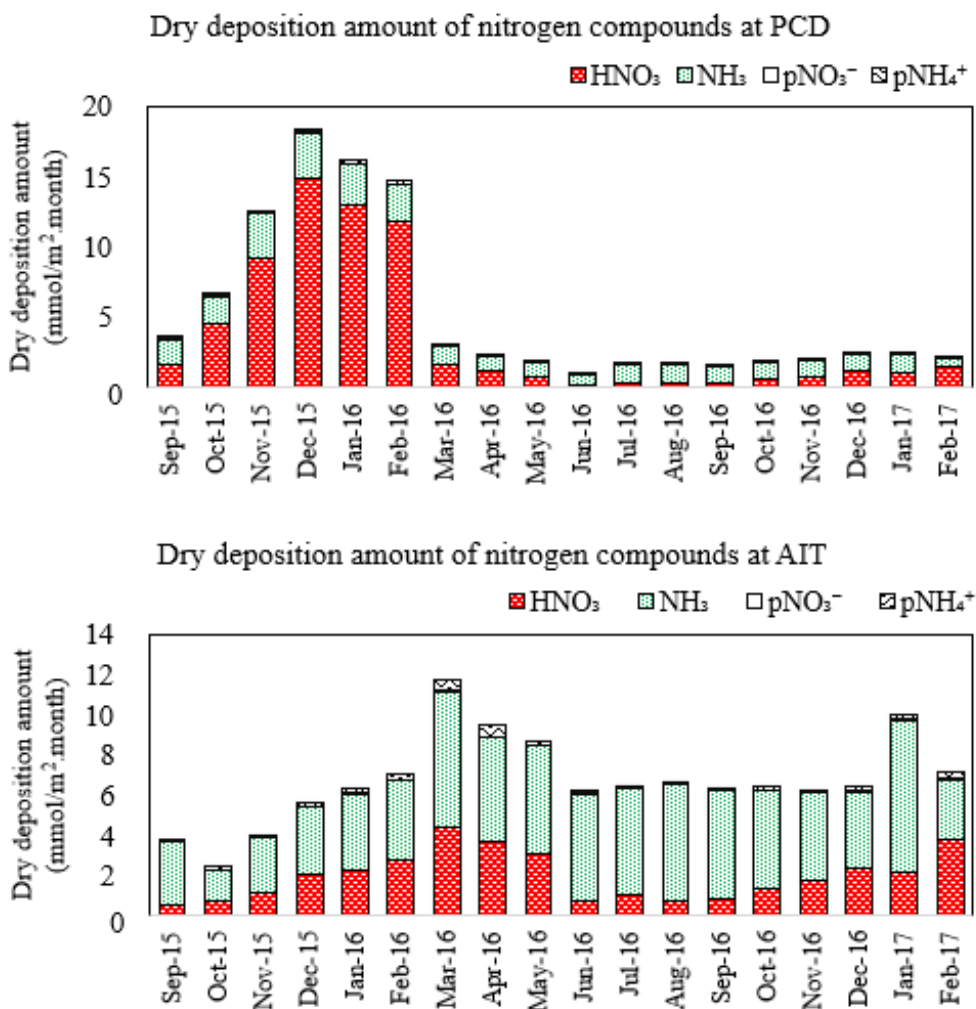


Figure 16. Monthly average dry deposition fluxes of nitrogen compounds at PCD and AIT sites

3.2.8 Comparison with the EANET data

Table 8 shows the comparison of the deposition results between this study and the EANET studies in BMR. For the wet deposition, the ranges were comparable except for Cl⁻ and K⁺ which were measured higher in our study for both sites. EANET data showed that most of parameters were measured higher at the downtown of Bangkok than in Pathumthani except for Ca²⁺ and Mg²⁺ that were in a close range. This study also showed that most of parameters were measured higher in PCD than AIT (SO₄²⁻, NO₃⁻, NH₄⁺, Na⁺, and Mg²⁺), especially NH₄⁺ and Mg²⁺ fluxes were significantly higher at PCD as compared to AIT. Note that the difference in the data period may be a reason for the difference in the fluxes, the results in this study quoted in Table 8 were for 2016 while that of EANET were the average of 5 years (2010-2014).

The dry deposition fluxes presented in Table 8 showed a drastic reduction of most of the fluxes between this study (measured in 2016) and those measured in the EANET in an earlier period (2005-2009). The reduction in SO₂ gas and particulate sulfate (pSO₄²⁻) fluxes may be attributed to the improvement in fuel quality used in the transportation sector (lower sulfur content). Especially, Euro4 was enacted in the year of 2012 and lower sulfur content in the fuel was required to be compatible to the Euro4 engine. Only HNO₃ fluxes

were almost the same in both studies. However, the EANET dataset showed that dry deposition fluxes were measured higher in the downtown than in Pathumthani except for pNH_4^+ while this study found that most of fluxes (SO_2 , NH_3 , pSO_4^{2-} , and pNH_4^+) were measured higher at AIT site than PCD site.

Table 8. Comparison of the Annual Average Wet, Dry Deposition, Gaseous and Aerosol Concentrations between this Study and EANET Study

Parameter	EANET data ^a		This study (2016) ^b	
	Bangkok	Pathumthani	PCD	AIT
Wet deposition ($\text{mmol/m}^2\cdot\text{yr}$)				
SO_4^{2-}	16.95	12.22	12.75	11.00
NO_3^-	36.24	26.58	27.19	27.25
Cl^-	14.03	12.42	20.4	22.43
NH_4^+	71.54	51.72	65.66	44.62
Na^+	13.59	11.38	13.54	13.48
K^+	3.17	2.68	12.45	13.12
Ca^{2+}	23.6	24.62	19.79	21.83
Mg^{2+}	2.82	2.98	5.19	1.70
SO_4^{2-}	16.95	12.22	12.75	11.00
Dry deposition fluxes ($\text{kg/km}^2\cdot\text{yr}$)				
SO_2	3,060	1,000	347	555
HNO_3	1,980	1,570	1,971	1,541
NH_3	2,674	1,744	304	1,081
pSO_4^{2-}	360	340	69	149
pNO_3^-	400	280	8	6
pNH_4^+	50	50	23	52
Gaseous and aerosol concentration (ppb and $\mu\text{g/m}^3$, or otherwise indicated)				
SO_2 (ppb)	0.8 - 7.3	0.3 - 1.8	2.1 ± 0.75 (0.31-3.83)	1.4 ± 0.64 (0.19-3.18)
HNO_3 (ppb)	0.5 - 1.0	0.3 - 0.8	1.0 ± 0.60 (0.11-3.49)	0.9 ± 0.54 (0.1-2.67)
NH_3 (ppb)	7.8 - 10.2	2.8 - 9.2	13.5 ± 2.84 (4.89-20.3)	15 ± 2.73 (5.99-21.26)
pSO_4^{2-} ($\mu\text{g/m}^3$)	2.13 - 4.71	1.39 - 4.69	2.8 ± 1.83 (0.02-11.27)	3.13 ± 1.81 (0.07-11.1)
pNO_3^- ($\mu\text{g/m}^3$)	1.44 - 2.83	0.52 - 2.02	0.42 ± 0.26 (0.08-1.79)	0.51 ± 0.25 (0.02-2.38)
pNH_4^+ ($\mu\text{g/m}^3$)	0.42 - 1.30	0.38 - 1.50	0.95 ± 0.65 (0.21-3.58)	1.17 ± 0.60 (0.03-3.64)

Note : ^a5-year averages during the period from 2010 to 2014 (wet deposition), 2005-2009 (dry deposition and aerosol), and , ^bAnnual average of 2016.

The average values of the gaseous and ionic PM concentrations are not available from the EANET dataset hence the comparison is not straightforward hence only the ranges are discussed here. For gaseous concentrations, HNO_3 and NH_3 concentrations were recorder higher than the EANET study while SO_2 was measured within similar ranges to the EANET. Aerosol ionic concentrations were also recorder higher for pSO_4^{2-} and pNH_4^+ while pNO_3^- was measured close to the ranges provided by the EANET. The time gap between these studies may be a reason for the difference.

3.3 Part 3: PM air quality dispersion model

3.3.1 Emission inventory for base year of 2015

This study updated EI for the base year of 2015 for the major source sectors of on-road traffic (Buadee, 2017), aviation (landing and take-off, LTO), crop residue and municipal solid waste OB, livestock, residential combustion and biogenic emission for the BMR domain. In addition, the emissions from loading and refuelling in fuel stations, power plants, oil tanks, farm machines, cremation were updated from the EI for the domain of 2010. The emission of industry (base year of 2013) was contributed by KMITL (Dr. Narisara Thongboonchoo, pers. Com.). The results of EI are presented in Table 9.

Table 9. Emission from Different Source Sectors in the BMR Domain, 2015 (t/yr)

Emission Source	NO _x	CO	NMVOC	SO ₂	NH ₃	PM ₁₀	PM _{2.5}	OC	BC
Aviation (LTO)	17,650	17,606	8,852	1,194	-	176	141	44	18
Biogenic	9,400	16,320	99,630	-	-	-	-	-	-
Crop residue OB	3,742	227,058	8,933	748	5,402	13,112	11,966	2,316	1,198
Cremation	15	6.8	0.6	26	-	0.7	-	-	-
Farm machine	121	71	32	0.001	-	19	18	3.7	5.6
Industry	53,251	134,284	14,674	90,725	-	8,669	1,858	867	223
Oil tank	-	-	980	-	-	-	-	-	-
Power plant	26,280	23,350	3,385	2,527	1,015	871	368	79	144
Residential	6,676	386,940	16,195	615	2,486	17,159	14,390	4,289	6,221
On-road transport	228,527	1,193,097	151,989	3,129	-	32,849	26,279	18,067	6,541
Livestock	-	-	-	-	10,893	-	-	-	-
MSW-OB	3,726	126,675	5,204	1,788	-	15,524	13,195	7,451	931
Gasoline station	-	-	6,878	-	-	-	-	-	-
Total Emission	349,387	2,125,408	316,754	100,752	19,796.5	88,380	68,216	33,119	15,282

Source: Pornsiri, 2017

The on-road transport sector contributed the most to the total emissions of NO_x, CO, NMVOC, PM₁₀, PM_{2.5}, BC and OC with the shares ranged from 37% to 65%. NH₃ emission was mainly contributed by livestock (55%) followed by crop residue OB (27%). SO₂ emission was mainly from industry (90%) followed by on-road transport of 3%. To conduct 3D air quality modelling using CAMx, speciated VOCs and particulate matter material (components) are required. An example of PM speciation (components) of the on-road mobile source compiled from the literature is presented in Table 10. The speciation was done for other sources using the VOC and PM profiles from US EPA SPECIATE and relevant literature sources. The spatial distributions of PM_{2.5} emissions (2 x 2 km²) of selected source sectors are presented in Figure 17.

Table 10 Speciated Emissions of PM from On-road Transport (Gg/yr)

Type of vehicle	PM ₁₀	PM _{2.5}	EC	OC	SO ₄ ⁻	NO ₃ ⁻	Other
On-road Gasoline Exhaust	20.20	13.13	2.50	7.21	0.11	0.02	3.30
LDDV Exhaust	10.60	6.89	3.54	2.45	0.06	0.02	0.83
HDDV Exhaust	0.94	0.61	0.47	0.11	0.002	0.0007	0.03

Note: PM speciation profile was taken from Subramanian et al. (2009) and US EPA SPECIATE.

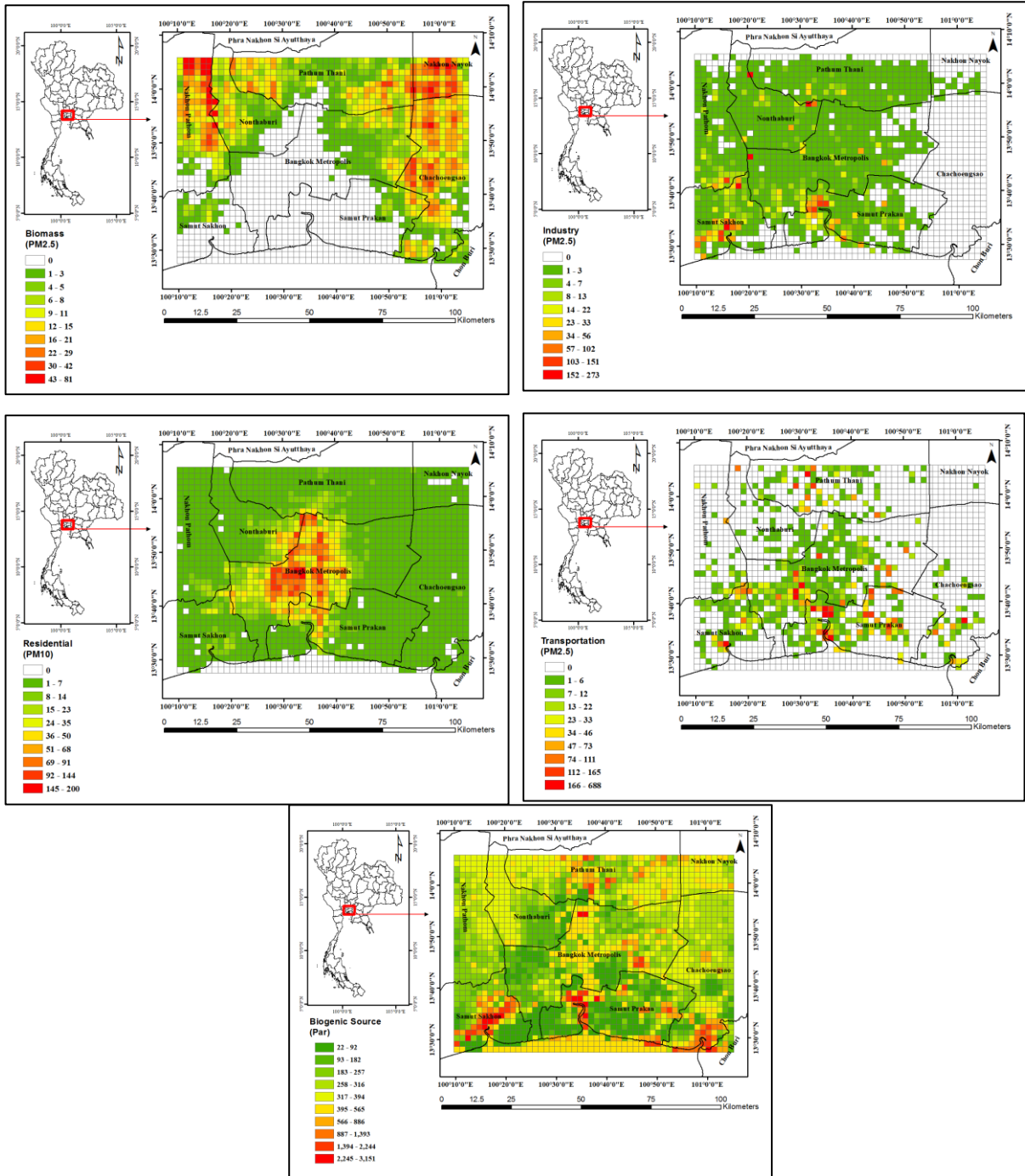


Figure 17. Spatial distribution of PM_{2.5} and biogenic VOC emissions from different source sectors in BMR (2 x 2 km²) in t/yr

The emissions from crop residue OB were distributed with higher intensity in the agricultural areas in Pathumthani, Nakhonpathom, Nakhonnayok, and Chacengsao while the emissions from industry were mainly concentrated in Samut Prakarn and Samut Sakhorn provinces. High emissions from the residential combustion were seen in the Bangkok city center due to the high population density. The transportation emissions were distributed along the main road networks where more driving activities with higher vehicle kilometre travelled (VKT) concentrated. Biogenic VOC emissions were intensive in the areas with high vegetation coverage and low in the city center of Bangkok.

The monthly emissions were derived from the monthly activity data, e.g. monthly fuel sale for traffic and fuel station, crop production for crop residue OB, monthly LTO for aviation, etc. Hourly emission profiles that are required for model running were obtained from the published profiles for the domain in Kim Oanh et al. (2014) which are presented in Figure 18.

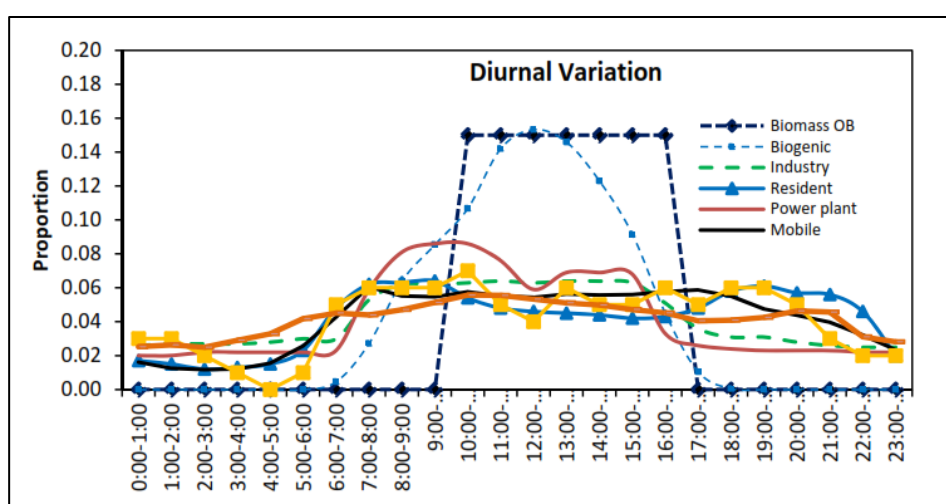


Figure 18. Temporal variation of other considered sources of BMR

3.3.2 WRF model performance evaluation

Statistical parameters used in the performance analysis consisted of the mean bias (MB), mean absolute gross error (MAGE), root mean squared error (RMSE) that were calculated for four parameters (temperature, wind speed, wind direction and relative humidity) and presented in Table 11. It can be seen that for temperature both criteria of MB and MAGE were fulfilled for November simulation for both stations. For wind speed, WRF reproduced reasonably well the observations at the DNM airport for both months, i.e. better than the performance for the SVN airport station. The model simulated satisfactorily for relative humidity, especially at DNM airport for which both criteria of MB and MAGE were met in both months. Overall, WRF performed reasonably in simulating all important meteorological parameters except for wind directions. The problems of wind direction simulations are normally related to the weak wind speeds hence the directions are highly variable. More WRF schemes should be tested to check the performance for this challenging parameter. When testing the “factor of 2” criteria the WRF performance however showed satisfactory performance for all parameters except for a slightly lower metric for the wind directions at SVN. The time series comparison between modelled temperature and wind speed with the respective observations are presented in Appendix 11. The scatter plots for temperature and relative humidity between the model results and observation are presented in Figure 19.

3.3.3 CAMx model performance evaluation

Statistical parameters used in the analysis consisted of Mean fractional bias (MFB) and Mean fractional error (MFE) calculated using the modelled and observed PM_{2.5} concentrations and results are presented in Table 12. The model underestimated the observed PM concentrations at the stations. For only MFB at 59T met the criteria for PM_{2.5}. The performance of model in simulating PM₁₀ was not better without any the statistical criteria seen satisfactorily. Several factors can affect the model performance including both the meteorological and the emission input data. Insufficiency of observed PM data is another issue. Further, the modelled results are grid average while the observed data are the point based hence cause the inconsistency in the comparison. Time series of modelled PM_{2.5} and PM₁₀ are presented in Appendix 11. The regular strikes of the hourly maximum of simulated PM were examined which show a strong influence by the low mixing height during the late afternoon (below 100 m). Further investigation should be done focusing on the Planetary Boundary Layer (PBL) physical options used in the WRF model.

Table 11 Summary of Statistical Performance of WRF in Selected Dry and Wet Month

Parameters	Temperature (°C)		Wind speed (m/s)		Wind direction (°)		Relative humidity (%)	
	DM	SVN	DM	SVN	DM	SVN	DM	SVN
August 2015								
N	671	671	607	615	673	673	738	738
MB	-1.30	-1.26	0.42	0.06	69.30	49.49	3.40	6.71
MAGE	1.98	1.78	1.30	1.34	90.20	85.33	9.63	9.21
RMSE	NE	NE	1.72	3.07	NE	NE	NE	NE
Factor of 2, in %	56	61.7	69	73.2	-	-	-	-
Wind directional accuracy, in %	-	-	-	-	67	52	-	-
November 2015								
N	691	690	604	604	673	673	673	673
MB	-0.02	0.41	-0.15	1.26	-8.38	-5.55	-5.09	-6.09
MAGE	0.99	1.08	1.18	1.82	114.15	57.71	6.24	7.51
RMSE	NE	NE	1.45	2.40	NE	NE	NE	NE
Factor of 2, in %	78	72	69	68	-	-	-	-
Wind directional accuracy, in %	-	-	-	-	58	56	-	-

Note: N – number of data, DM – Don Mueang, SVN – Survanabhumi,

The bolded values show meeting of compliance to the criteria provided by Emery et al. (2001).

Wind speed: MB $\leq \pm 0.5$ m/s, RMSE ≤ 2 m/s;

Wind direction: MAGE ≤ 30 deg, MB $\leq \pm 10$ deg;

Temperature: MAGE ≤ 2 °K, MB $\leq \pm 0.5$ °K;

Humidity: MAGE ≤ 2 g/kg, MB $\leq \pm 1$ g/kg.

Factor of two (Temperature): 60%,

Factor of two (wind speed): 50%,

Directional accuracy: 55-65%.

Taking the advantage of the measurement data of PM compositions produced in this project a comparison between the modelled output and the was also conducted. Modelled hourly PM_{2.5} mass concentrations and compositions (i.e. PSO_4^{2-} , PNO_3^- , BC, and OC) in November 2015 were used to compute the weekly average to compare with the available

weekly monitoring at two sites (AIT and PCD sites described above). At the PCD site, the height of measurement was 64 m high (at the roof top) thus model results were extracted for the layer 3 with sigma pressure of 0.99. At the AIT site, the height was 6 m, hence model results used for the comparison were those extracted for the lowest layer. The results are presented in Table 13 for both sites.

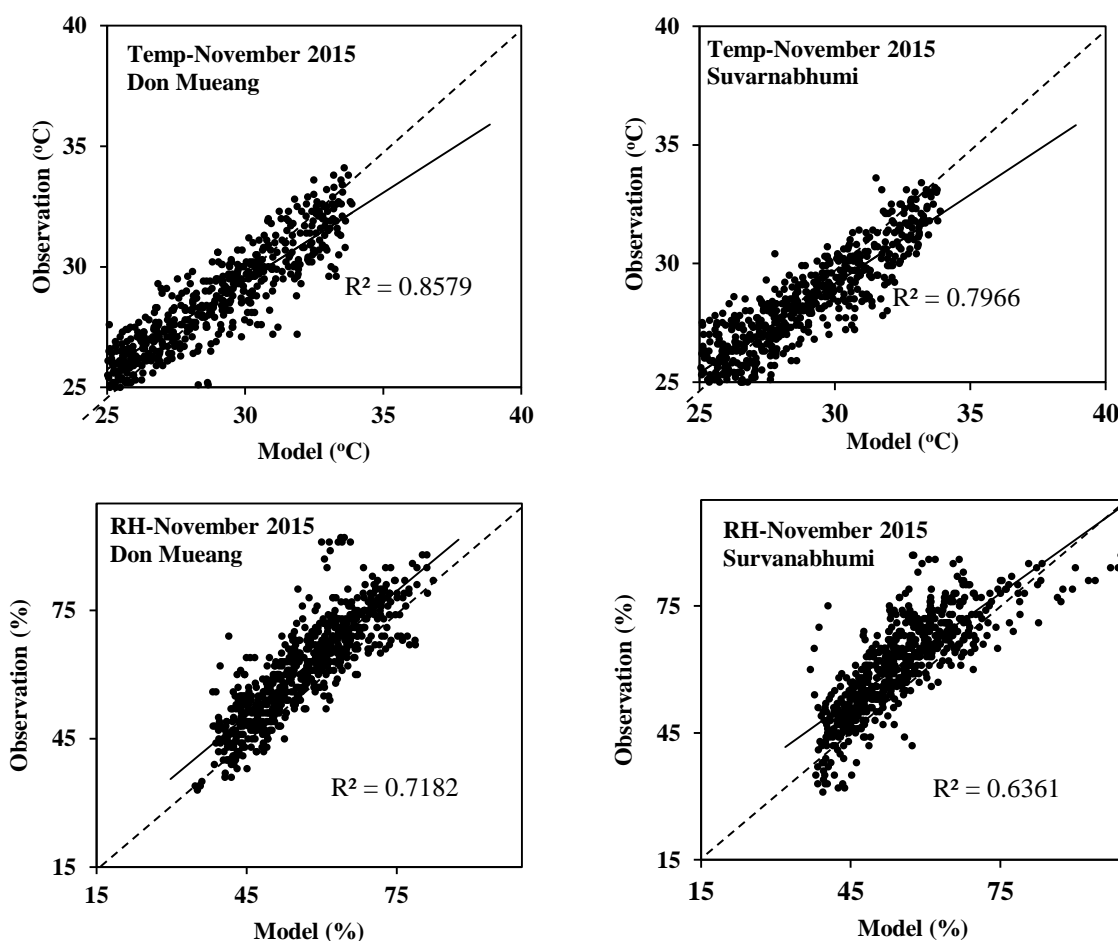


Figure 19. Scatter plots between the hourly modeled and observed temperature and RH (relative humidity) for August and November 2015 in SVN and DNM stations

At both sites, the weekly average $PM_{2.5}$ concentrations showed more comparable results between the modelled and observed than for the case of hourly measurements (PCD monitoring data). However, at PCD the simulated $PM_{2.5}$ concentrations were lower than the observation for the first two weeks but were higher for the last 2 weeks of November 2015. The simulated pNO_3^- concentrations were consistently higher than the observed while others (i.e. pSO_4^{2-} , BC and OC) were lower (Table 13). However, the modelled and observed concentrations appear to be of the same magnitude.

At the AIT site, the modelled $PM_{2.5}$ mass concentrations were mostly higher than the observed values. For the PM components, the model overestimated pNO_3^- , but underestimated the pSO_4^{2-} , BC and OC levels. During November month, the site was potentially affected by the rice straw open burning which commonly occur in the surrounding area. Further, the discrepancy in PM composition may come from the

simulation of the secondary organic aerosol (SOA) formulation which generally poses a large uncertainty. There may be other sources of primary PM such as wind-blown dust, unpaved road, and sea salt emissions which were not considered in this simulation. In addition, the PM speciation for the source sectors needs to be improved using the locally generated source profiles. Model performance evaluation for August will be conducted in the future study for 2016 base year in which the project monitoring data is available.

Table 12 Statistical Analysis of CAMx Model Performance of Hourly PM_{2.5}

Statistical Measure	27T	59T	54T
PM_{2.5}			
August			
N	714	709	706
Mean Fraction Bias (MFB)	-110	-53	-102
Mean Fraction Error (MFE)	125	92	115
November			
N	648	697	675
Mean Fraction bias	-154	-96	-105
Mean Fraction error	157	109	128
PM₁₀			
August			
N	385	396	402
Mean Fraction Bias (MFB)	-128	-118	-126
Mean Fraction Error (MFE)	133	120	130
November			
N	396	396	396
Mean Fraction bias	-135	-128	-147
Mean Fraction error	140	134	149

Note: ST-27 (Samut Sakhon, ambient), 54T (Dindaeng, roadside), and 59T (Public Relation Department, ambient)

Bold: Satisfied the criteria

Suggested Criteria: MFB = $\leq 60\%$

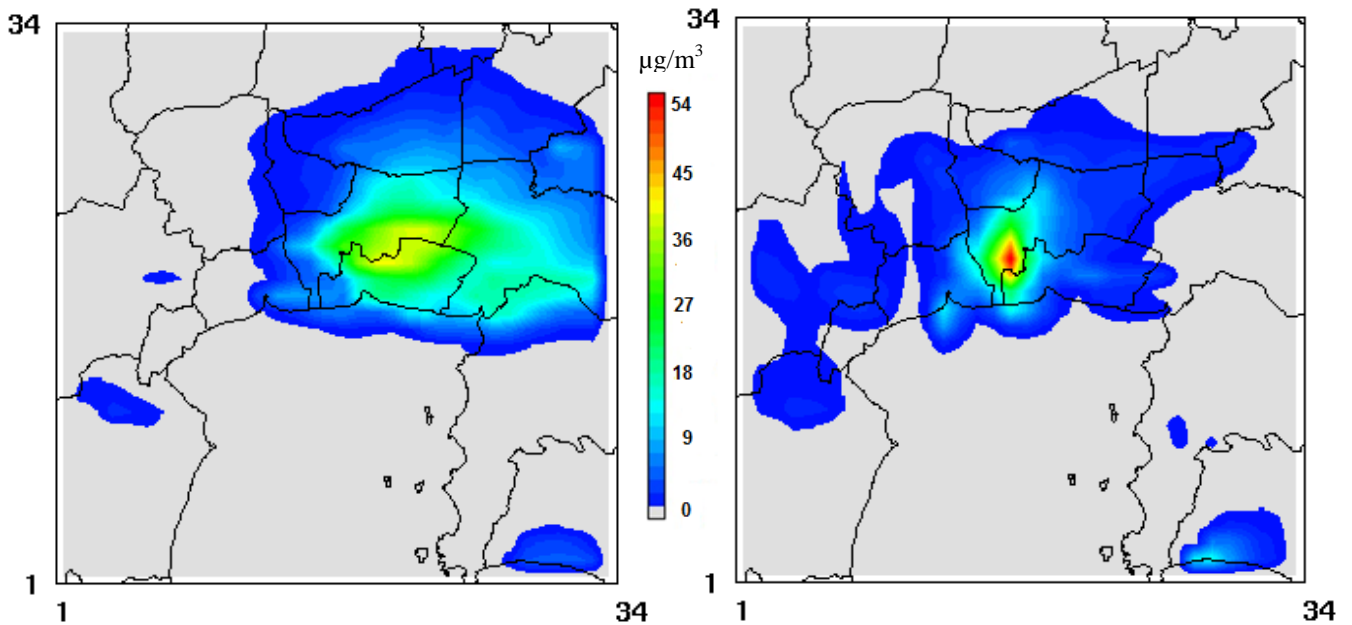
MFE = $\leq 75\%$ 3.3.4 Simulated fields of PM_{2.5} in BMR

The monthly average PM_{2.5} mass concentrations fields are presented in Figure 20 for the CENTHAI domain in August and November 2015. The highest concentrations in the domains were concentrated in the city center where the traffic activity was intensive. The domain maximum value of monthly average concentration was higher in November ($54 \mu\text{g}/\text{m}^3$) as compared to August ($40 \mu\text{g}/\text{m}^3$). This was expected because of more intensive emission from crop residue OB in the dry month of November along with less precipitation hence less wet removal in the month. The hourly maximum concentrations of simulated PM_{2.5} for the BMR domain in August and November 2015 are presented in Figure 21. As expected, domain maximum hourly value in November ($131 \mu\text{g}/\text{m}^3$) was higher than in August ($118 \mu\text{g}/\text{m}^3$). The PM_{2.5} plume moved to the NE-E direction in August following the SW monsoon while in November the plume moved to the SW direction following the NE monsoon direction.

Table 13 Weekly Modeled vs. Observed PM_{2.5} and its Composition at PCD and AIT Sites

Period of sampling	PM _{2.5} (µg/m ³)		PSO ₄ ²⁻ (µg/m ³)		PNO ₃ ⁻ (µg/m ³)		BC (µg/m ³)		OC (µg/m ³)	
	O	M	O	M	O	M	O	M	O	M
PCD site										
2-9 November 2015	22.59	16.34	3.94	0.96	0.34	2.87	3.94	1.09	4.53	2.46
9-16 November 2015	22.43	19.16	3.45	1.02	0.82	3.30	4.55	1.37	4.22	3.12
16-23 November 2015	21.45	23.29	3.62	2.21	1.04	2.65	3.55	1.49	4.91	4.14
23-30 November 2015	14.50	20.50	3.03	1.75	0.50	3.12	4.07	1.44	5.81	4.14
Average	20.24	19.82	3.51	1.48	0.67	2.98	4.03	1.35	4.87	3.47
AIT site										
2-9 November 2015	16.55	18.16	2.33	1.06	0.30	3.19	3.69	1.22	4.13	2.74
9-16 November 2015	24.62	20.13	3.39	1.07	0.93	3.47	4.43	1.44	4.52	3.28
16-23 November 2015	21.89	31.89	2.81	3.02	0.32	3.63	4.10	2.05	5.82	5.67
23-30 November 2015	20.87	29.25	2.42	2.50	0.40	4.45	3.96	2.05	5.27	5.90
Average	20.98	24.86	2.74	1.91	0.49	3.68	4.04	1.69	4.93	4.40

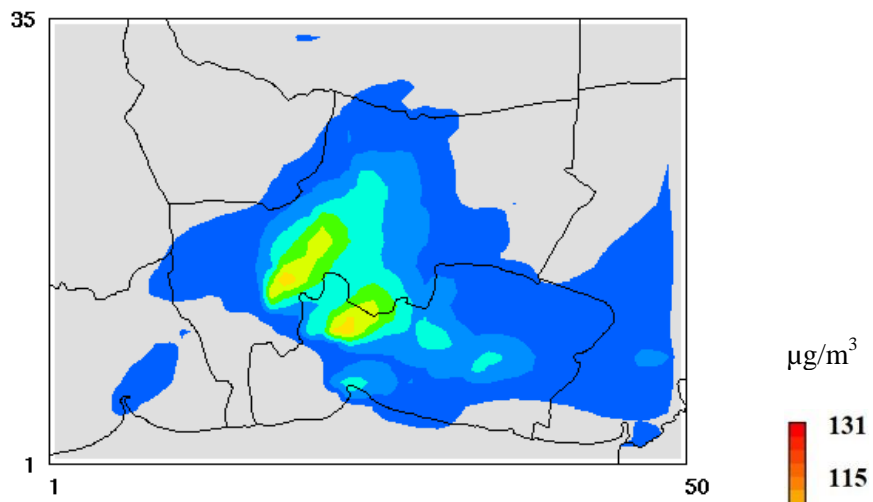
Note: O – observed, M – modelled



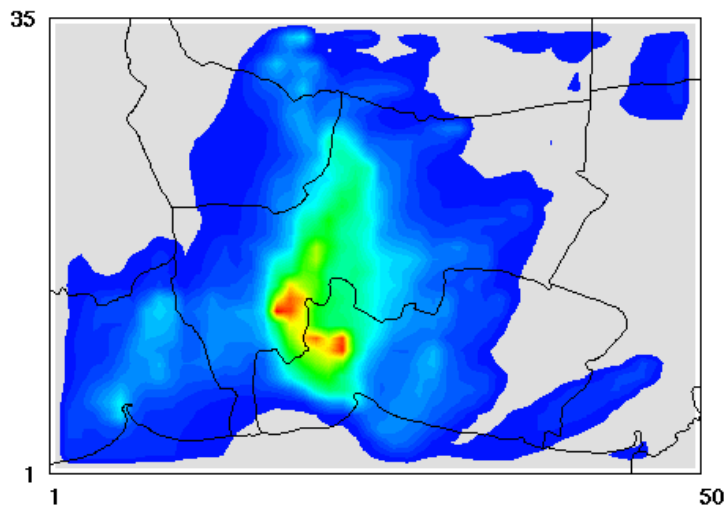
a) CENTHAI, August 2015

b) CENTHAI, November 2015

Figure 20. Monthly average of simulated PM_{2.5} in the CENTHAI domain in August and November 2015



c) 24 August, 17:00 LST



d) 18 November, 18:00 LST

Figure 21. Hourly maximum of simulated PM_{2.5} in BMR domain in August and November 2015

4. CONCLUSION AND RECOMMENDATION

4.1 Summary and Conclusions

This final report presents the key findings of the project activities for the period of March 2015 – December 2017. The monitoring was conducted during the period from September 2015 until February 2017 for PM mass, composition and acid deposition monitoring. The source apportionment for PM, emission inventory and PM dispersion modelling results are presented.

4.1.1 Particulate matter mass and compositions

- The PM mass concentrations measured at the city center and suburban sites were comparable for both fine and coarse fractions. In the wet period, PM_{2.5} and PM_{>2.5} mass concentrations measured at AIT site ($15 \pm 5 \mu\text{g}/\text{m}^3$ and $37 \pm 16 \mu\text{g}/\text{m}^3$) were almost the same as those measured at PCD ($15 \pm 6 \mu\text{g}/\text{m}^3$ and $38 \pm 16 \mu\text{g}/\text{m}^3$). However, in the dry period, the suburban site even had higher average PM levels, i.e. PM_{2.5} and PM_{>2.5} at AIT site (32 ± 11 and $44 \pm 18 \mu\text{g}/\text{m}^3$) that were slightly higher than PCD (28 ± 10 and $41 \pm 15 \mu\text{g}/\text{m}^3$) which may be the effects of rice straw OB around the site. The annual average PM_{2.5} was higher at AIT ($24.8 \mu\text{g}/\text{m}^3$) than PCD ($22.2 \mu\text{g}/\text{m}^3$) which were approaching the annual NAAQS of $25 \mu\text{g}/\text{m}^3$ suggesting urgent need for the emission reduction to revert the trend.
- The portion of PM_{2.5} in the total SPM (PM_{2.5}+PM_{>2.5}), expressed by the ratio between PM_{2.5} and SPM, was also mostly similar at the 2 sites. At PCD, the ratio was 0.30 and 0.42 in the wet and dry period, respectively, while at AIT it was 0.31 and 0.43, respectively. Higher ratios in the dry period when the PM levels were also high showed the increase in the secondary formation, more biomass OB emissions along with the less wet removal of the fine PM.
- Carbonaceous aerosol made up a relatively large fraction of PM_{2.5}. The average EC and OC concentrations in PM_{2.5} were respectively $2.75 \pm 1.44 \mu\text{g}/\text{m}^3$ and $4.29 \pm 3.34 \mu\text{g}/\text{m}^3$ at PCD and $3.60 \pm 2.19 \mu\text{g}/\text{m}^3$ and $5.52 \pm 4.59 \mu\text{g}/\text{m}^3$ at AIT. The levels of EC and OC were lower in the coarse PM, i.e. EC and OC in PM_{>2.5} were $0.84 \pm 0.55 \mu\text{g}/\text{m}^3$ and $1.80 \pm 0.67 \mu\text{g}/\text{m}^3$, respectively, at PCD while the corresponding levels at AIT were $1.07 \pm 0.57 \mu\text{g}/\text{m}^3$ and $2.40 \pm 1.97 \mu\text{g}/\text{m}^3$. The wet period had lower EC and OC concentrations than the dry period at both sites.
- At both sites, the most dominant anion in PM_{2.5} was SO₄²⁻ in both wet and dry periods that was, respectively, $2.49 \mu\text{g}/\text{m}^3$ and $3.22 \mu\text{g}/\text{m}^3$ at PCD, and $2.37 \mu\text{g}/\text{m}^3$ and $4.10 \mu\text{g}/\text{m}^3$ at AIT. NH₄⁺ was the major cation in PM_{2.5} at both sites that was $0.79 \mu\text{g}/\text{m}^3$ in the wet period and $1.41 \mu\text{g}/\text{m}^3$ in dry period at PCD, and $1.55 \mu\text{g}/\text{m}^3$ in the wet period and $0.78 \mu\text{g}/\text{m}^3$ in the dry period at AIT.
- The ion balance analysis showed more basic ions (as compared to acidic) in PM_{2.5} in both sites and during both dry and wet periods with strong linear correlations between the sum of cations and the sum of anions (in $\mu\text{eq}/\text{m}^3$). The ion balance for the coarse fraction (PM_{>2.5}) was less consistent than that for PM_{2.5}. The analysis for organic ions and other inorganic ions (such as carbonate) should be done to improve the ion balance for both PM fractions.

4.1.2 Source apportionment results

- The reconstructed mass results showed that the major PM_{2.5} mass group at both sites in both dry and wet periods were OM-biomass which suggested a strong influence of the biomass open burning emissions on the PM mass concentrations.
- The CMB results showed consistent important source factors at both sites of biomass OB, diesel vehicles, secondary inorganic PM and industry. The biomass OB contribution was the most dominant in the dry season while the vehicle emission was most dominant in the wet season. In dry period, at PCD, the most important contributors to PM_{2.5} were biomass burning (35%), and diesel vehicles (21%) and those at AIT were also biomass burning (36%), diesel vehicles (26%), inorganic secondary PM (15%) and industry (5%). In the wet period, at PCD, the most important contributors to PM_{2.5} were diesel vehicles (28%), biomass burning (26%) and inorganic secondary PM (21%). At AIT the most significant contributors were also diesel vehicles (28%), biomass burning (24%) and inorganic secondary PM (23%).
- High PM weeks in February 2017 recorded at both sites were characterized by a regional pathway of air mass trajectory originated from the continental part of SEA following the NE monsoon direction to arrive at the sites hence indicating a potential of long range transport of pollution. The low PM weeks at both sites in October 2016 were associated with the marine pathway of air mass before arriving to the sites which brought in a relatively clean air mass to the monitoring sites following the prevailing SW monsoon direction.

4.1.3 Acid deposition

- The average pH of rainwater at PCD and AIT were in range between 4.6 – 7.1 and 4.7 – 7.0, respectively, and the average pH in dry period was lower than wet period.
- The average electrical conductivity at PCD and AIT were 2.02 ± 1.11 and 2.08 ± 1.65 mS/m, respectively, also with higher values during the dry period due to lower precipitation amount hence more concentration of the chemical species in the rain water.
- The total wet deposition fluxes of individual species at both PCD and AIT were ranging between 5.3 to 86.1 meq/m² and followed a similar rank as follows: NH₄⁺>Ca₂⁺>NO₃⁻>SO₄²⁻>Cl⁻>Na⁺>K⁺>Mg²⁺.
- The concentrations of acidic gases measured at both sites were ranging between 0.6 to 13.5 ppb and ranked as follows: NH₃ > SO₂ > HNO₃ > HCl.
- The dry deposition fluxes (calculated for both gases and PM acidic components using the resistance method) were smaller than the wet deposition, especially during the rainy months. This showed that the wet deposition played an important role to remove sulfur and nitrogen species from the atmosphere.
- The total sulfur deposition in 2016 was 586 kg/km².yr while that of the nitrogen deposition was 2,235 kg/km².yr. The total deposition fluxes of S and N were still lower than the critical loads suggesting that there was less potential risk at present for the terrestrial ecosystem in Pathumthani.

4.1.4 Emission inventory and PM air quality dispersion modeling

- On-road transport sector contributed the most to the total emissions of NO_x, CO, NMVOC, PM₁₀, PM_{2.5}, BC and OC (37 to 65%) while NH₃ emission was mainly from

livestock (55%) and SO₂ emission was mainly from industry (90%). The spatial distribution of the emissions of each sector showed consistent patterns, for example, with the activity data with higher emission intensity of traffic along the major road networks in the domain.

- The meteorological model of WRF showed a satisfactory performance with the “Factor of 2” criteria met for most parameters. The statistical criteria evaluation for WRF showed more satisfactory performance for temperature and relative humidity than for wind speed and wind directions. Weak winds with variable directions in the domain remain a challenge to simulate.
- WRF-CAMx simulation results of PM_{2.5} showed higher concentrations in November than August which agreed with the observed data.
- WRF-CAMx model system underestimated the hourly PM_{2.5} measured at 3 PCD automatic stations in 2015. However, the model performance evaluation using the weekly-based monitoring results conducted within this JICA project showed more reasonable agreement.

4.2 Recommendation

Technical recommendations:

1. Further studies should continue the monitoring activities to better characterize the PM mass and composition that can be used to improve the PM source apportionment. Long term data of the acid deposition can be used to assess its potential impacts on the ecosystem in the domain.
2. The ambient datasets at both sites should be further scrutinized and the estimation of the uncertainty should be made to prepare better input for receptor modelling using more advanced statistical models of PMF and Multilinear Engine (ME). More complete elemental composition should be included in the model input. Gaseous concentrations and meteorological observations can be included in the ME modelling input to produce better source apportionment results.
3. The CMB source apportionment results should be further improved by including additional local source profiles for both fine and coarse PM, such as domestic cooking and solid waste open burning. A comparative analysis of the results of several models, i.e. CMB, PMF and ME, may provide better insight in to the quantitative contributions of the major sources to the PM pollution at both urban and suburban areas of BMR.
4. Analysis for other PM components, such as organic ions, and organic compounds of levoglucosans and polycyclic aromatic hydrocarbons (PAHs) would provide more information on the contributing sources and improve the ion balance for the PM.
5. Emission inventory data should be updated and PM speciation should be done using regional specific measurements (e.g. using regional specific source profiles) to improve the input data for the PM dispersion modelling.
6. Meteorological model performance should be improved especially for wind speed and wind direction by applying several physical options for WRF modelling. The model performance evaluation should be done for mixing height and by use also other large-scale data such as satellite observations.
7. The PM simulation should be conducted for the whole year in the base case and also for scenario emissions to analyse the co-benefits of the policy intervention on the air quality, health impact, and climate forcing reduction in the domain.

Policy recommendations:

1. The emission reductions should be focused on the key sources contributing to PM in BMR of traffic and biomass OB.
2. The emission reduction for vehicles can be achieved by the means of implementation of progressive stringent engine standard for vehicles and fuel technologies and by applying an age limit for vehicles to remove the old and polluting vehicles from the streets, etc.
3. The emissions from the biomass open burning (mainly rice straw field burning in BMR) can be controlled by introducing alternative measures that can be effectively accepted by farmers to opt for non-burning alternatives along with implementation of strict regulations.
4. Emissions from the industry should be controlled focusing on PM, PM precursors, and air toxics.
5. The air quality management system should be improved by: i) adding more stations for PM_{2.5} monitoring in both urban and sub-urban areas, ii) continuously updating the emission inventory, and iii) using modelling tools to assess co-benefits of emission reduction scenarios on air quality improvement, health impact and climate forcing reductions.

5. REFERENCE

- Boylan, J. W., & Russell, A. G. (2006). PM and light extinction model performance metrics, goals, and criteria for three-dimensional air quality models. *Atmospheric Environment*, 40(26), 4946-4959.
- EANET - Acid Deposition Monitoring Network in East Asia. (2010). *Guidelines for acid deposition monitoring in East Asia*. Retrieved from <http://www.eanet.asia/product/guideline/monitorguide.pdf>
- EANET - Acid Deposition Monitoring Network in East Asia. (2013). *Technical Manual for Air Concentration Monitoring in East Asia*. Retrieved from <http://www.eanet.asia/product/manual/techacm.pdf>
- EANET - Acid Deposition Monitoring Network in East Asia. (2015). *Review on the State of Air Pollution in East Asia*. Retrieved from <http://www.eanet.asia/product/RSAP/RSAP.pdf>.
- Emery, C., Tai, E., & Yarwood, G. (2001). *Enhanced meteorological modeling and performance evaluation for two Texas ozone episodes*. CA, USA: ENVIRON International Corporation.
- Kim Oanh, N.T., Pongkiatkul, P., & Upadhyay, N., (2009). Designing ambient particulate matter monitoring program for source apportionment study by receptor modeling. *Atmospheric Environment*, 43, 3334-3344.
- Kim Oanh, N.T., Pongkiatkul, P., Upadhyay, N., & Hang, N.T., (2014). Monitoring Particulate Matter Levels and Composition for Source Apportionment Study in Bangkok Metropolitan Region. *Improving Air Quality in Asian Developing Countries*. (pp.151, 173).
- Kim Oanh, N.T., Pongkiatkul, P., Cruz, M.T., Dung, N.T., Philip, L., et al. (2013). Chapter 3: monitoring and source apportionment for particulate matter in six Asian cities. Ed. By Nguyen Thi Kim Oanh, CRC Press, Boca Raton, Florida, USA (pp. 97, 124).
- Kim Oanh, N. T., Permadi, D. A., Kingkeaw, S., Chatchupong, T., & Pongprueksa, P. (2014). Study of ground-level ozone in Bangkok Metropolitan Region by advanced mathematic modeling for air quality management. Bangkok: Asian Institute of Technology.
- Shrestha, R. M., Kim Oanh, N.T., Shrestha, R., Rupakheti, M., Permadi, D.A., Kanabkaew, T., Salony, R. (2013). Atmospheric Brown Cloud (ABC) Emission Inventory Manual (EIM), United Nation Environmental Programme (UNEP), Nairobi, Kenya.
- Ostro, B., Chestnut, L., Vichit-Vadakan, N., & Laixuthai, A., (1999). The Impact of Particulate Matter on Daily Mortality in Bangkok, Thailand. *Air and Waste Management Association*, 49, 100-107
- Vichit-Vadakan, N., & Vajannapoom, N. (2010). Health impact from air pollution in Thailand: Current and future challenges. *Environ Health Perspectives*, 119(5), 197-198.

APPENDICES

Appendix 1 QA/QC of IC analysis

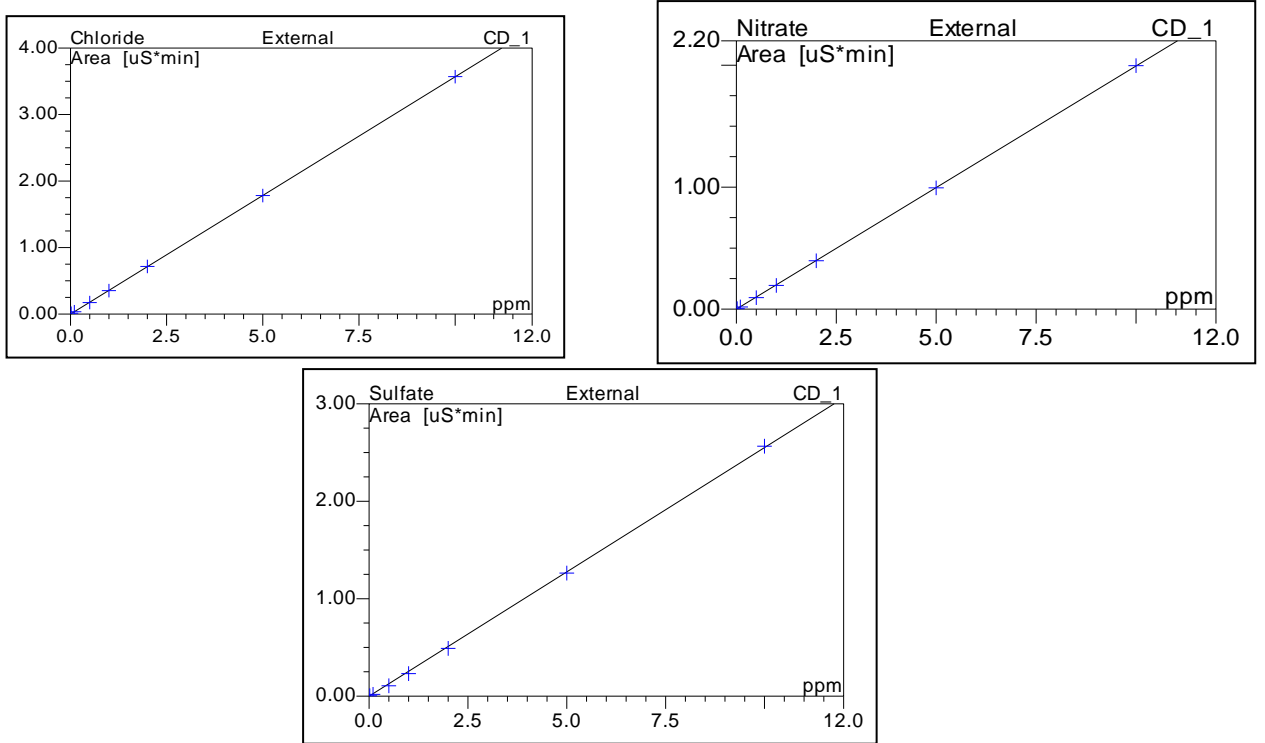


Figure A1.1 Anions calibration graphs

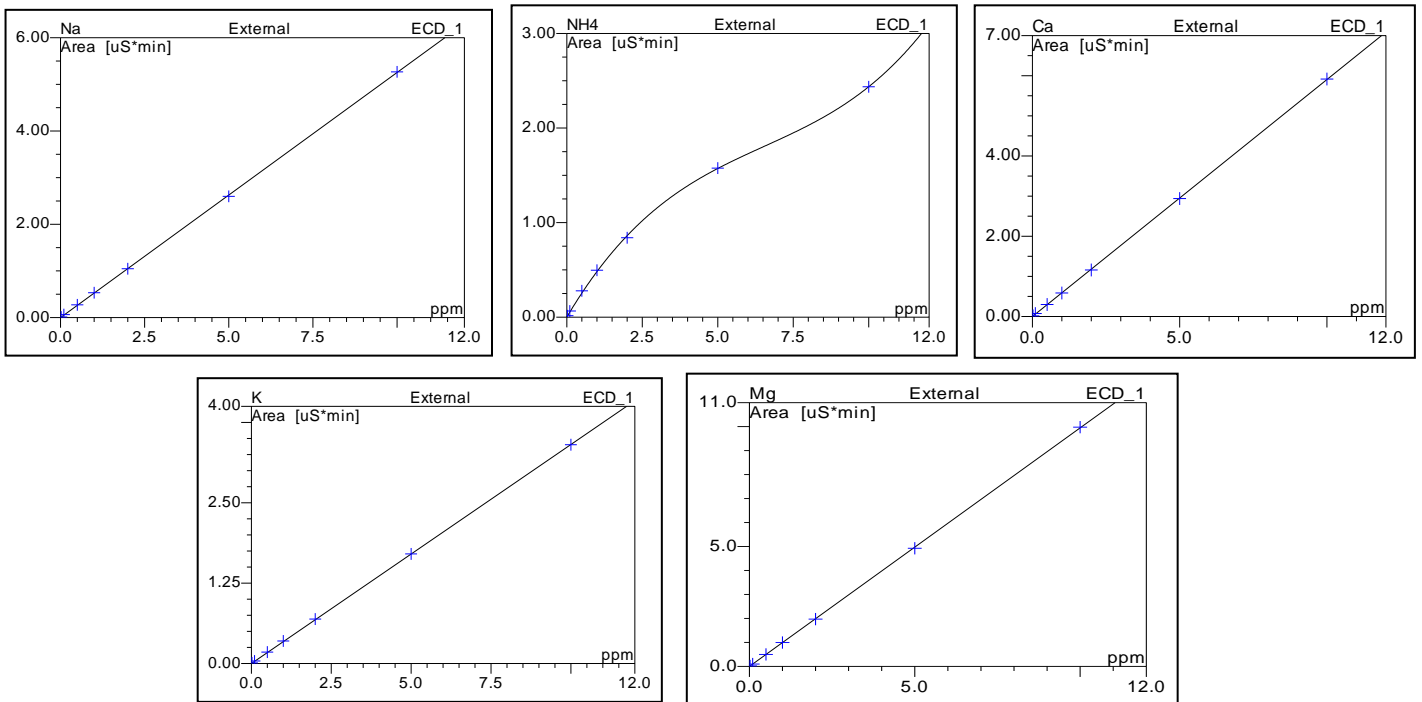


Figure A1.2 Cations calibration graphs

Table A1.1 Calibration for Cations Species

No.	Ret.Time min	Peak Name	Cal.Type	Points	R-Square %	Offset	Slope	Curve
1	4.46	Na	Lin	7	0.999945	0.0000	0.5254	0.0000
2	5.03	NH4	Cubic	7	0.999703	0.0000	0.5394	-0.0604
3	6.13	K	Lin	7	0.999973	0.0000	0.3406	0.0000
4	9.12	Mg	Lin	7	0.999958	0.0000	0.9950	0.0000
5	10.81	Ca	Lin	7	0.999963	0.0000	0.5906	0.0000
Average:					0.9999	0.0000	0.5982	-0.0121

Table A1.2 Calibration for Anions Species

No.	Ret.Time min	Peak Name	Cal.Type	Points	R-Square %	Offset	Slope	Curve
6	4.98	Chloride	Lin	7	0.999990	0.0000	0.3568	0.0000
8	7.38	Nitrate	Lin	7	0.999968	0.0000	0.1993	0.0000
11	11.72	Sulfate	Lin	7	0.999656	0.0000	0.2551	0.0000
Average:					0.9999	0.0000	0.2704	0.0000

Appendix 2.1 Methodology of calculation of weighted average concentrations

The weighted average concentrations of components in rain water were determined as follows:

$$C_{Ai} (\mu\text{eq/L}) = \frac{\sum C_i P_i}{\sum P_i} \quad (\text{Eq. 1})$$

Where,

C_{Ai} : ion concentration ($\mu\text{eq/L}$)
 P_i : precipitation amount (mm)

The wet deposition fluxes were determined using the following equation:

$$\text{Wet deposition flux } (\mu\text{eq/m}^2) = \frac{C_{Ai} \times V}{A} \quad (\text{Eq. 2})$$

Where,

V : rain volume (L)
 A : area of glass funnels (m^2); $A = \pi r^2$
 r : radius of glass funnel (100 mm)

The concentrations of gas and aerosol components in the air were basically determined as follows (EANET, 2013):

$$C_{\text{Air}} = \alpha \times \text{net } C_{\text{Sol}} \times V_{\text{Sol}} / V_{\text{Air}} \quad (\text{Eq. 3})$$

Where,

C_{Air} : concentration in the air (nmol/m^3)
 $\text{net } C_{\text{Sol}}$: net concentration in the solution (mg/l)
 V_{Sol} : volume of the solution (ml)
 V_{Air} : volume of the sampled air corrected at 20 °C, 1 atm (m^3)
 α : $10^3 / M$ with M is molecular weight (g/mole)

The net concentration in the solution was calculated as follows:

$$\text{net } C_{\text{Sol}} = C_{\text{Sol, Sample}} - C_{\text{Sol, Blank}} \quad (\text{Eq. 4})$$

Where,

$C_{\text{Sol, Sample}}$: concentration in the solution from the sample filter (nmol/m^3)
 $C_{\text{Sol, Blank}}$: concentration in the solutions from the blank filter (nmol/m^3).

A deposition flux was calculated from the air concentration and deposition velocity (EANET, 2010).

$$F_i = V_d^i \times C_i \quad (\text{Eq. 5})$$

Where,

F_i : flux of i species (nmol/m^2)
 C_i : concentration of i species (nmol/m^3)
 V_d^i : deposition velocity of i species (m/s)

Appendix 2.2 Meteorological conditions

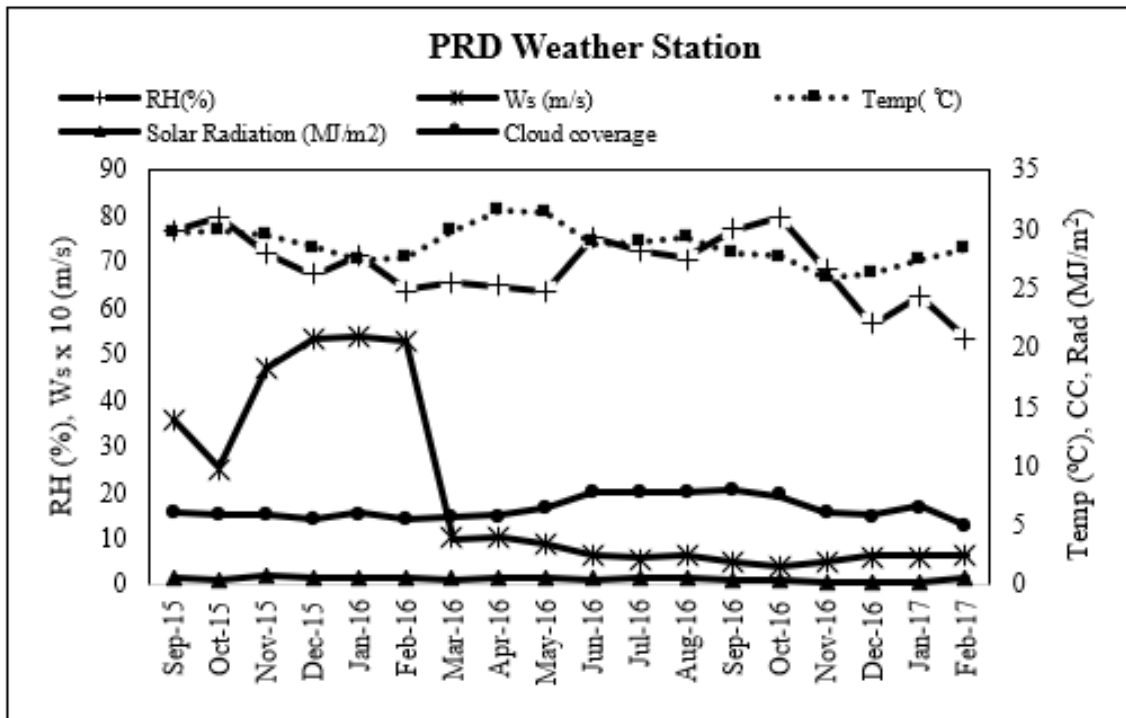


Figure A.2.2.1 Monthly average meteorological data at PRD weather station for PCD site

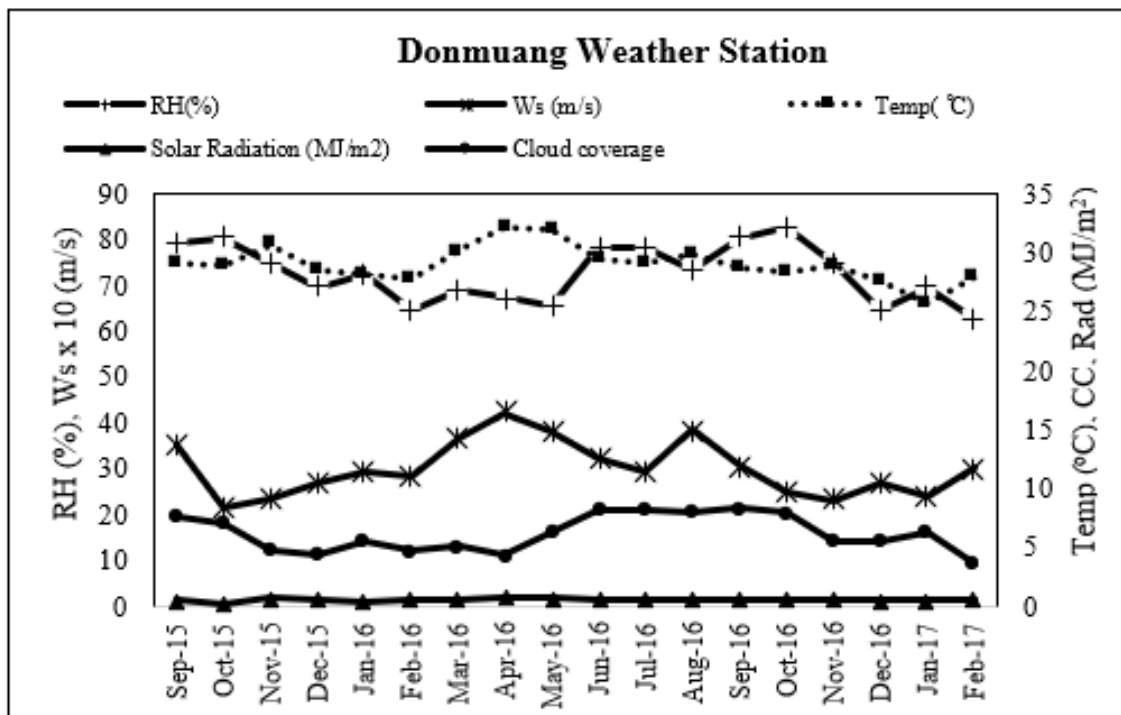


Figure A.2.2.2 Monthly average meteorological data at Donmuang weather station for AIT site

Appendix 3 Summary of EC/OC concentrations PM_{2.5} and PM_{>2.5} in dry and wet period at AIT and PCD

Site	Period	PM _{2.5} (µg/m ³)			PM _{>2.5} (µg/m ³)		
		EC	OC	EC/TC ratio	EC	OC	EC/TC ratio
PCD	Wet	1.5 ± 3.2 (0.05-8.51)	2.5 ± 6.1 (0.49-13.52)	0.37	1.3±0.2 (1.05-1.65)	2.1±0.2 (1.75-2.46)	0.38
	Dry	3.2 ± 1.2 (1.06-5.62)	6.1 ± 3.0 (0.83-12.63)	0.34	0.9 ± 0.6 (0.08-2.10)	1.9 ± 0.7 (0.74-3.28)	0.32
AIT	Wet	2.4 ± 0.9 (0.59-5.28)	2.5 ± 1.7 (0.9-8.3)	0.49	1.3±0.3 (0.41-1.3)	2.2 ± 0.6 (1.11-2.33)	0.37
	Dry	4.7 ± 2.5 (0.07-14.66)	8.5 ± 4.6 (0.50-24.39)	0.35	1.2 ± 0.7 (0.15-2.25)	2.9 ± 2.7 (0.37-15.53)	0.29

Appendix 4 Ion balance

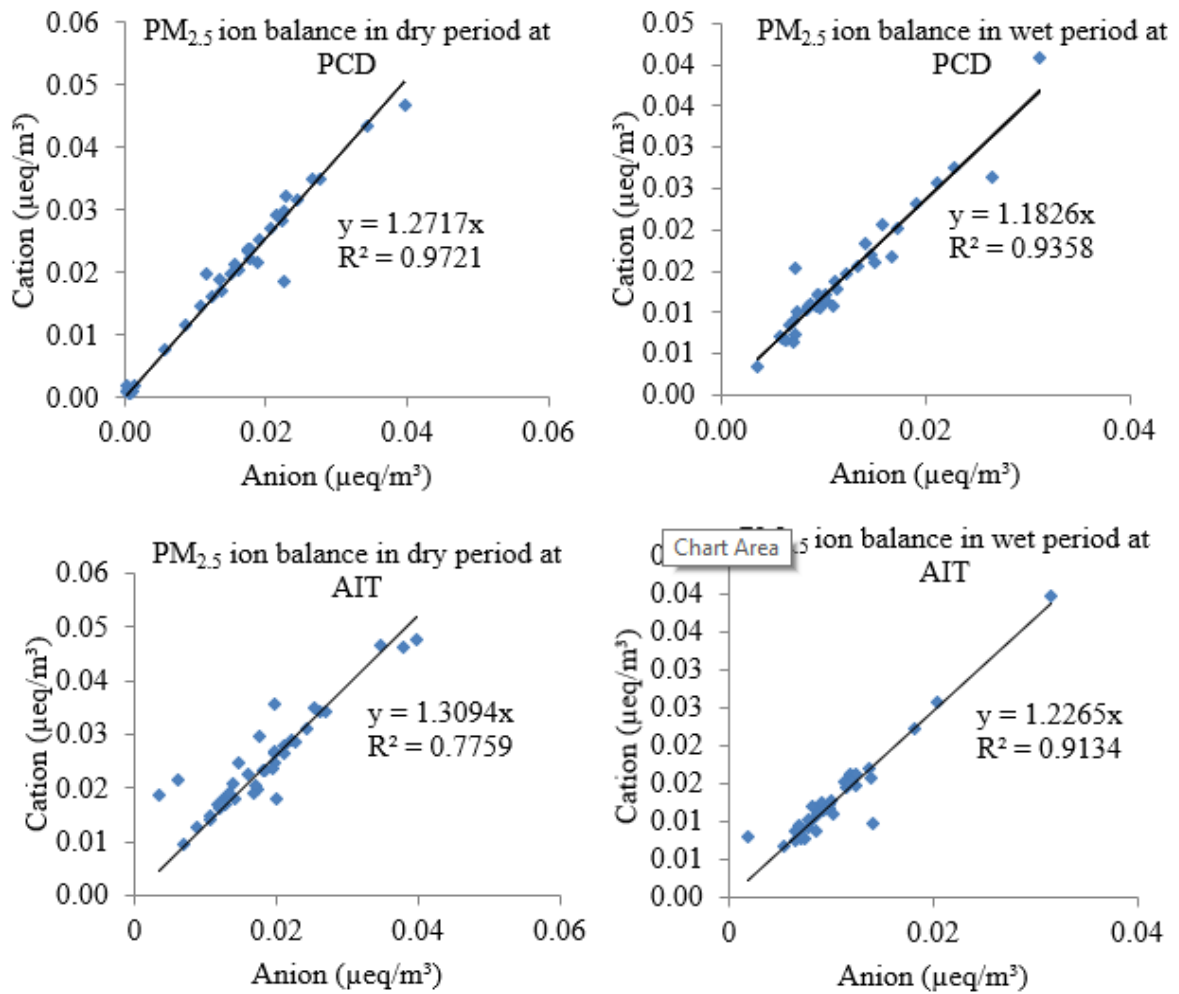


Figure A4.1 Ion balance for PM_{2.5} in wet and dry period at PCD and AIT sites

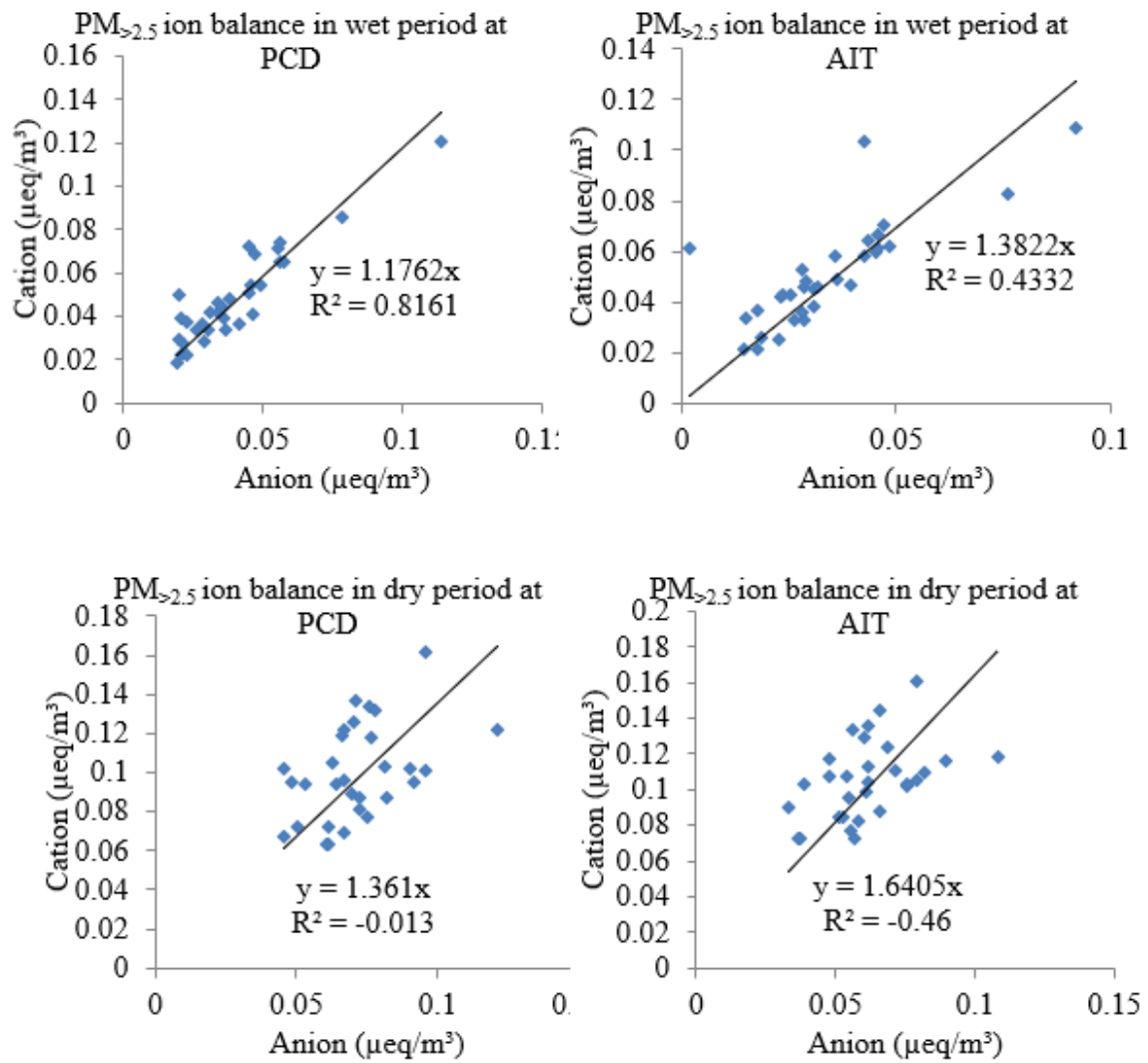
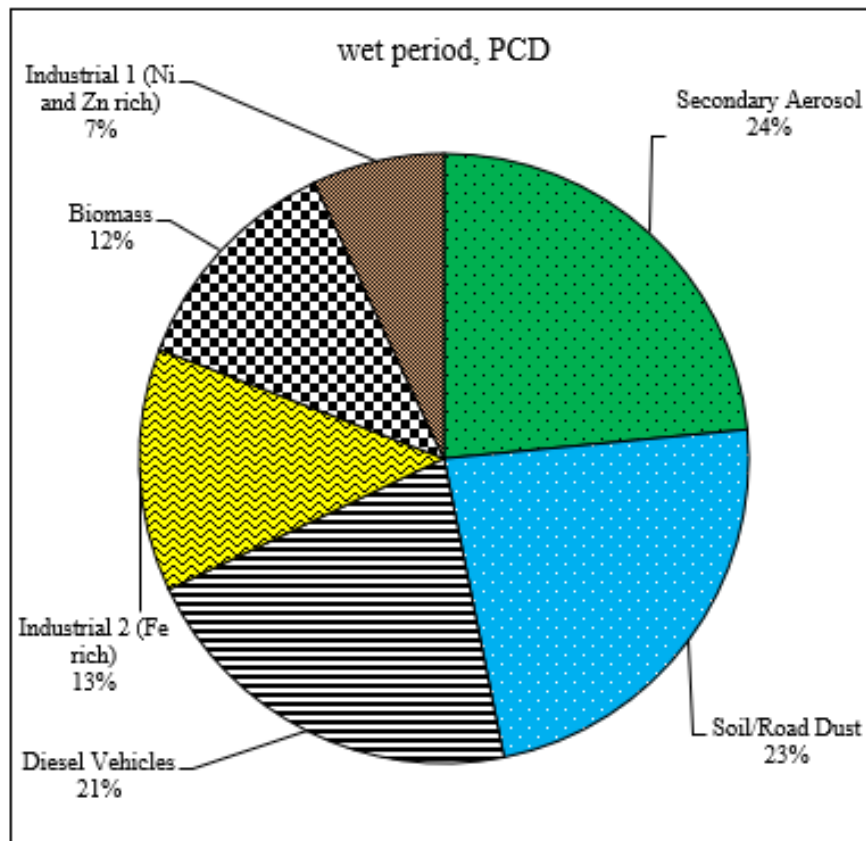


Figure A4.2 Ion balance for PM_{>2.5} in wet and dry period at PCD and AIT sites

Appendix 5. Example of average source contributions to PM_{2.5} in wet period, PCD by PMF



Appendix 6. HYSPLIT backward trajectory results

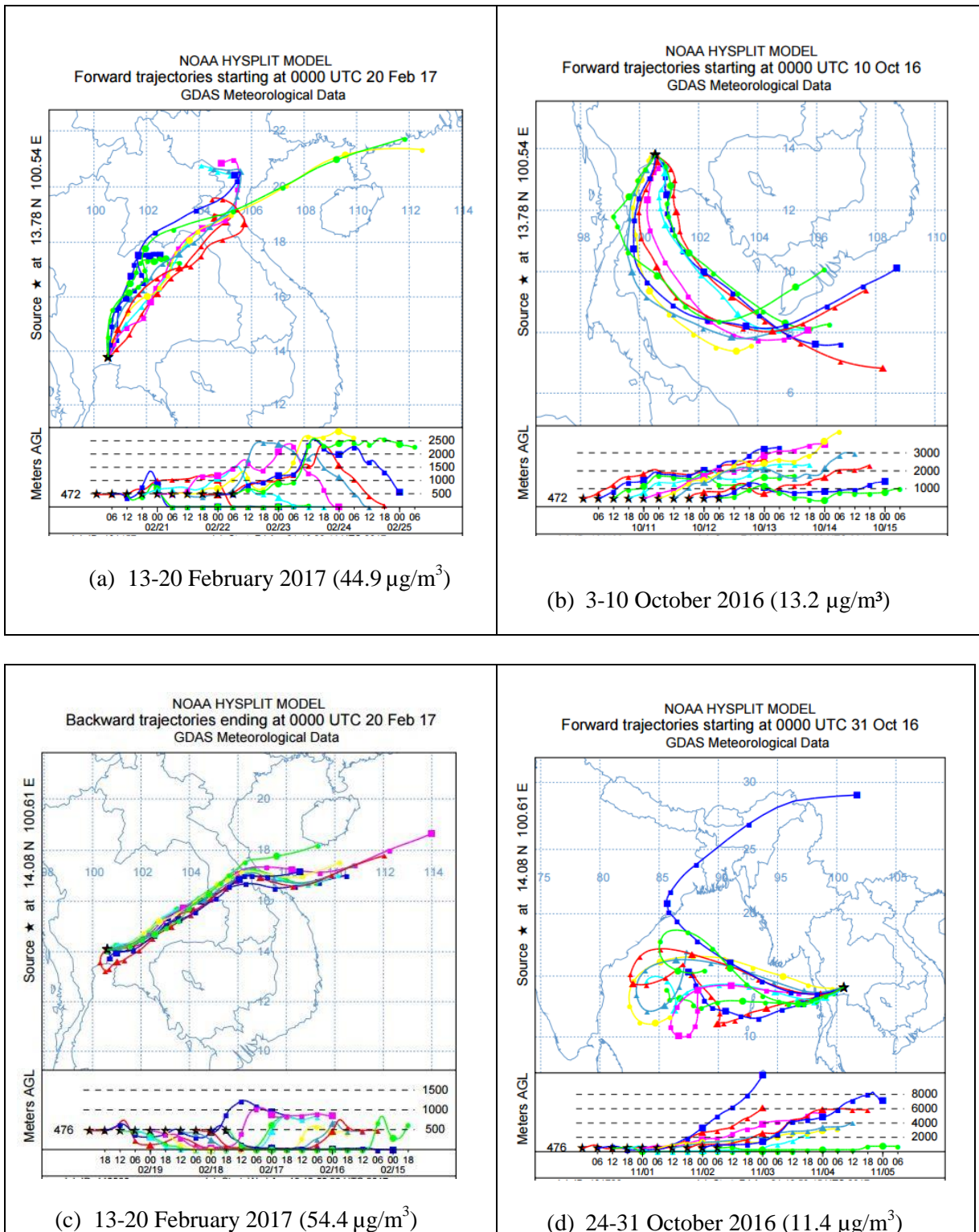
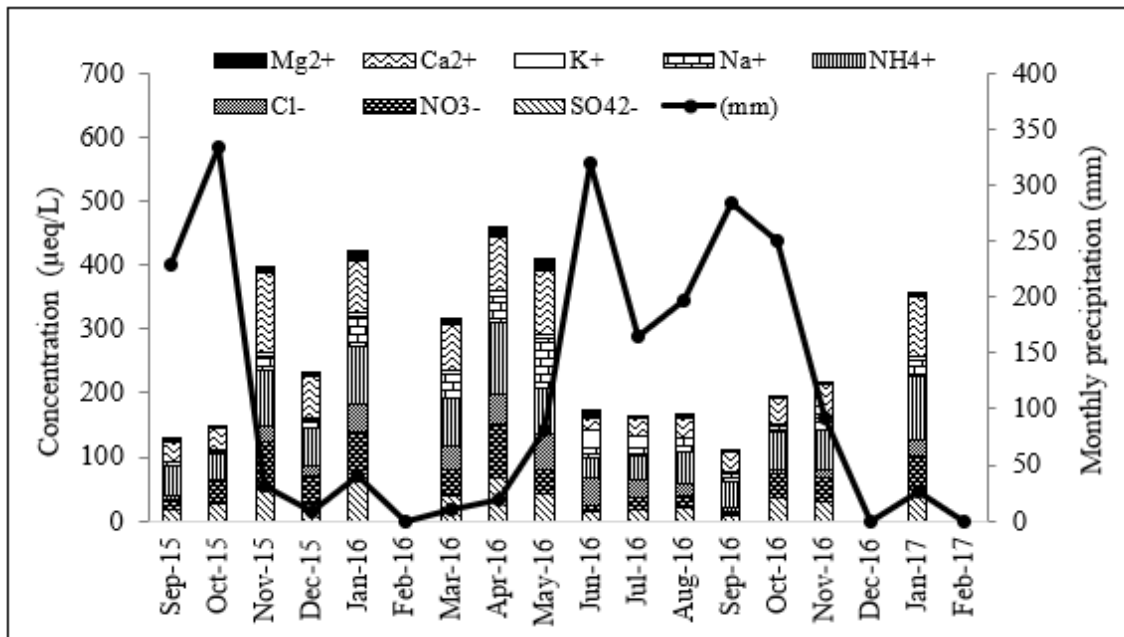
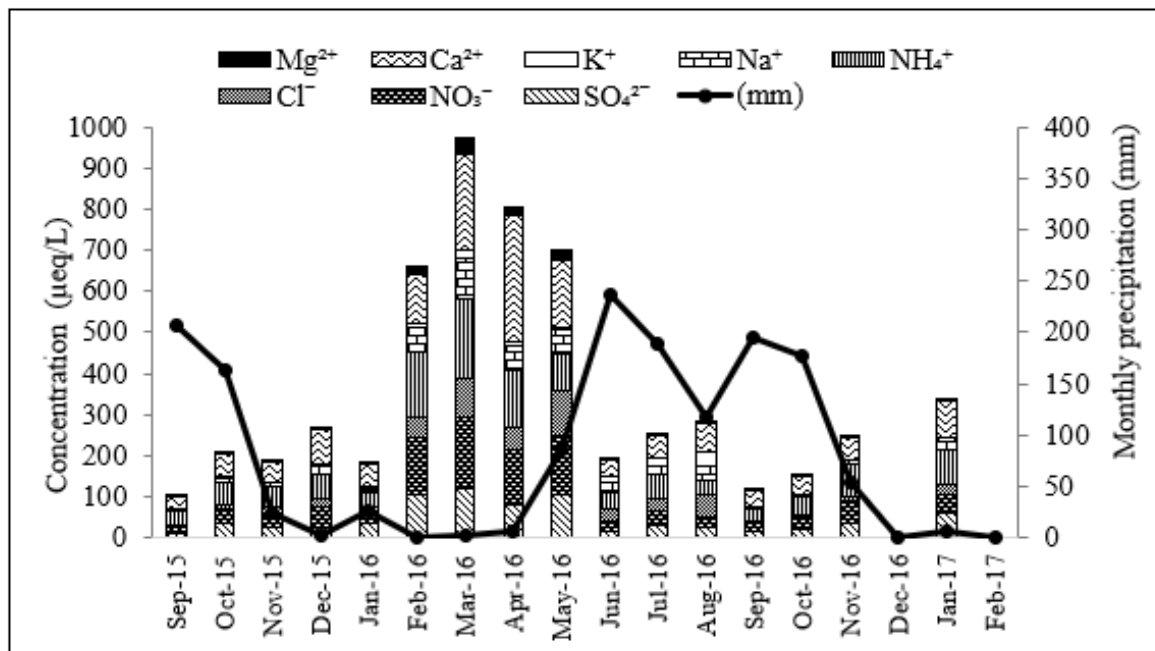


Figure A6.2 HYSPLIT backward trajectories to PCD and AIT on February 2017 and October 2016.

Appendix 7 Weighted monthly average concentrations at both sites



a) PCD site



b) AIT site

Appendix 8 Monthly average concentration of PM components (ionic species)

Month	Monthly average concentration of particulate matter($\mu\text{g}/\text{m}^3$)					
	PCD			AIT		
	pSO_4^{2-}	pNO_3^-	pNH_4^+	pSO_4^{2-}	pNO_3^-	pNH_4^+
Sep-15	1.39	0.37	0.40	1.64	0.30	0.54
Oct-15	4.26	0.56	1.57	1.76	0.41	1.05
Nov-15	2.78	0.66	1.03	2.87	0.55	0.93
Dec-15	3.50	0.85	1.35	1.37	0.72	1.30
Jan-16	4.01	0.49	1.42	3.92	0.64	1.44
Feb-16	5.09	0.64	1.76	5.01	0.80	1.74
Mar-16	6.19	0.33	2.16	6.36	0.49	2.23
Apr-16	6.05	0.14	2.01	7.91	0.24	2.60
May-16	2.71	0.29	0.94	3.00	0.29	1.00
Jun-16	1.31	0.31	0.26	1.80	0.57	0.50
Jul-16	1.72	0.35	0.47	1.77	0.25	0.54
Aug-16	2.40	0.58	0.63	2.29	0.44	0.58
Sep-16	2.05	0.44	0.65	1.94	0.28	0.59
Oct-16	3.49	0.32	1.04	3.54	0.17	1.16
Nov-16	2.55	0.95	1.02	2.48	0.32	0.80
Dec-16	0.66	0.14	0.28	1.37	0.72	1.30
Jan-17	0.13	0.05	0.05	2.91	0.91	0.98
Feb-17	0.16	0.04	0.06	4.36	1.00	1.71
Average	2.80	0.42	0.95	3.13	0.51	1.17
SD	1.83	0.26	0.65	1.81	0.25	0.60

Appendix 9 QA/QC of acid deposition results

A9.1 Ion level in the blanks

Lot Number	Polyamide Filter (F1)				Alkali Filter (F2)		Acid Filter (F3)
	SO ₄ ²⁻	NO ₃ ⁻	Cl ⁻	NH ₄ ⁺	SO ₄ ²⁻	Cl ⁻	NH ₄ ⁺
Lot1	0.007	0.167	0.412	0.004	0.034	0.062	0.091
Lot2					0.027	0.084	0.063
Lot3					0.023	0.062	0.068
Lot4	0.008	0.044	0.263		0.031	0.110	0.194
Lot5					0.040	0.077	0.157
Lot6					0.049	0.077	0.135
Lot7	0.027	0.059	0.293	0.010	0.101	0.219	0.054
Lot8					0.147	0.212	0.043

Table A9.2 Values of pH, EC and Ions in the Artificial Rain Samples No.141w, No. 142w, and Analytical Results

Each parameter		pH	EC (mS/m)	SO ₄ ²⁻ (μmol/l)	NO ₃ ⁻ (μmol/l)	Cl ⁻ (μmol/l)	Na ⁺ (μmol/l)	K ⁺ (μmol/l)	Ca ²⁺ (μmol/l)	Mg ²⁺ (μmol/l)	NH ₄ ⁺ (μmol/l)
141 W	Analyzed value	4.5	3.1	48.4	37.8	54.0	45.1	6.9	23.5	10.1	47.8
	Certified value	4.7	3.2	49	37.1	54.8	44.8	6.9	24.7	10.1	48.6
	Allowable value	4.0- 5.4	2.7- 3.7	41.7- 56.4	31.5- 42.7	46.6- 63.0	38.1- 51.5	5.9- 7.9	21.0- 28.4	8.6- 11.6	41.3- 55.9
	Percentage difference	4.3	2.5	1.2	-1.9	1.5	-0.7	0.0	4.9	0.0	1.6
142 W	Analyzed value	4.9	1.3	21.7	17.1	17.3	15.9	3.0	10.4	4.1	24.3
	Certified value	5	1.39	22.1	17	18	14	3.2	9.9	3.9	24.4
	Allowable value	4.3- 5.8	1.2- 2.6	18.8- 25.4	14.5- 19.6	15.3- 20.7	11.9- 16.1	2.7- 3.7	8.4- 11.4	3.3- 4.5	20.7- 28.7
	Percentage difference	2.0	3.6	1.8	-0.6	3.9	-13.6	6.3	-5.1	-5.1	0.4

A9.3 Ion balance (R_1) and Conductivity agreement (R_2)

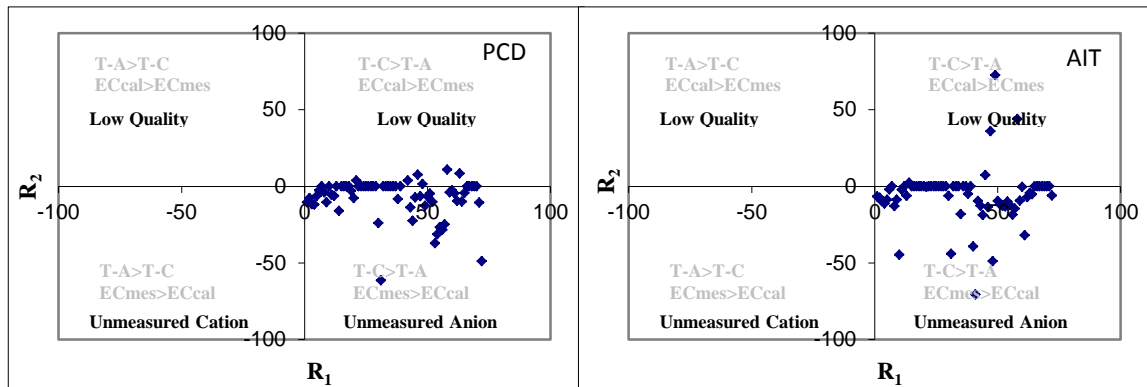


Figure A9.3.1 Relationship between R_1 and R_2 at PCD and AIT sites

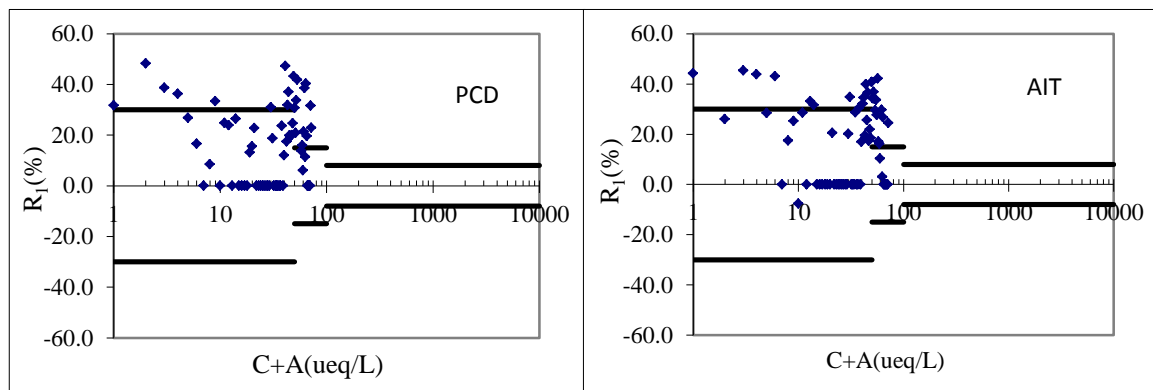


Figure A9.3.2 Ion balance of rain samples collected at two sampling sites during September 2015 - February 2017

Table A9.4 Results of Ion Balance and Electrical Conductivity Agreement

Name of sites	Sample (N)	R_1 (N)	R_1 (AA)	%	R_2 (N)	R_2 (AA)	%	R_1 & R_2 (N)	R_1 & R_2 (AA)	%
PCD	45	45	3	6.7	43	34	79.1	43	2	4.7
AIT	43	43	3	7.0	43	34	79.1	43	2	4.7

Note:

(N): Number of samples

R_1 (N): Number of samples measured and calculated ion balance (R_1)

R_1 (AA): Number of samples within allowable ranges for R_1

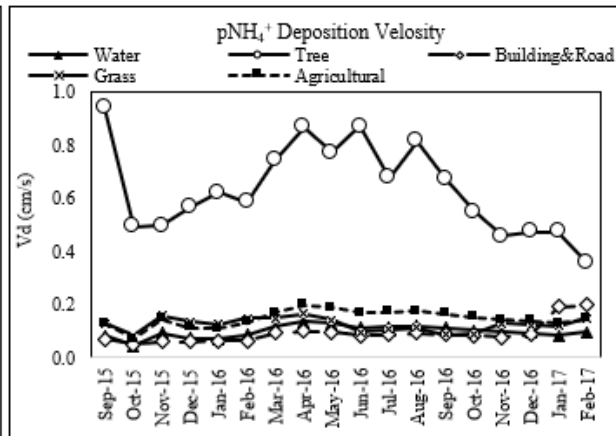
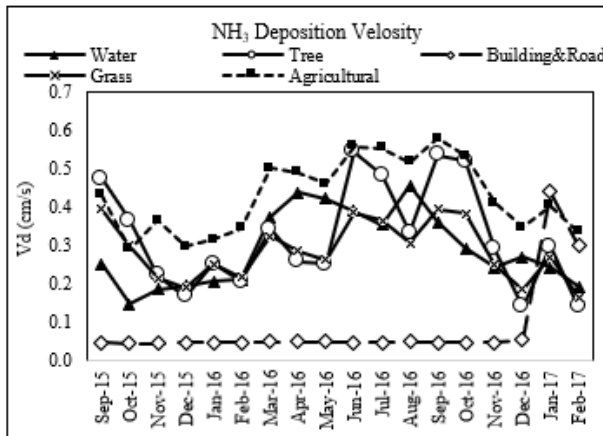
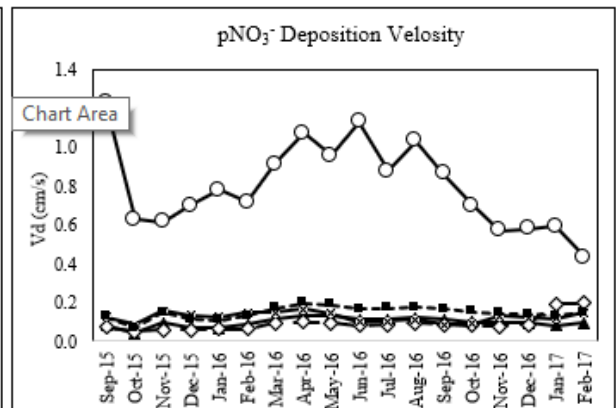
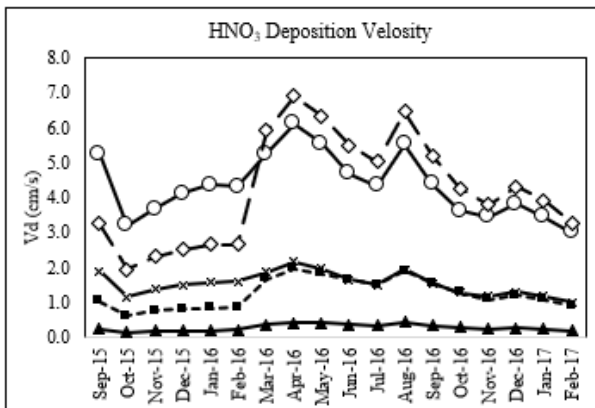
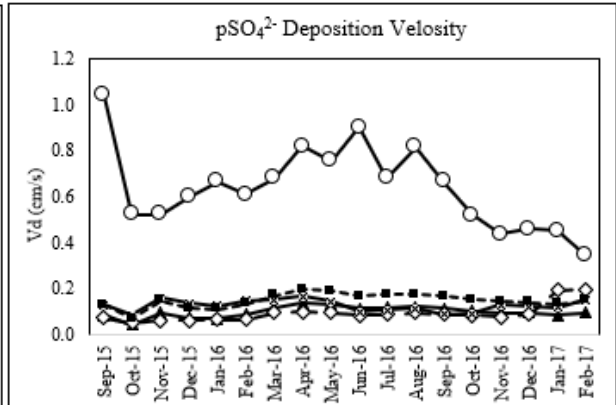
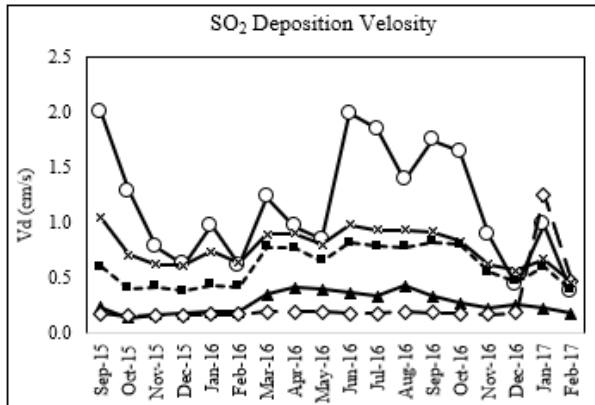
R_2 (N): Number of samples measured and calculated conductivity agreement (R_2)

R_2 (AA): Number of samples within allowable ranges for R_2

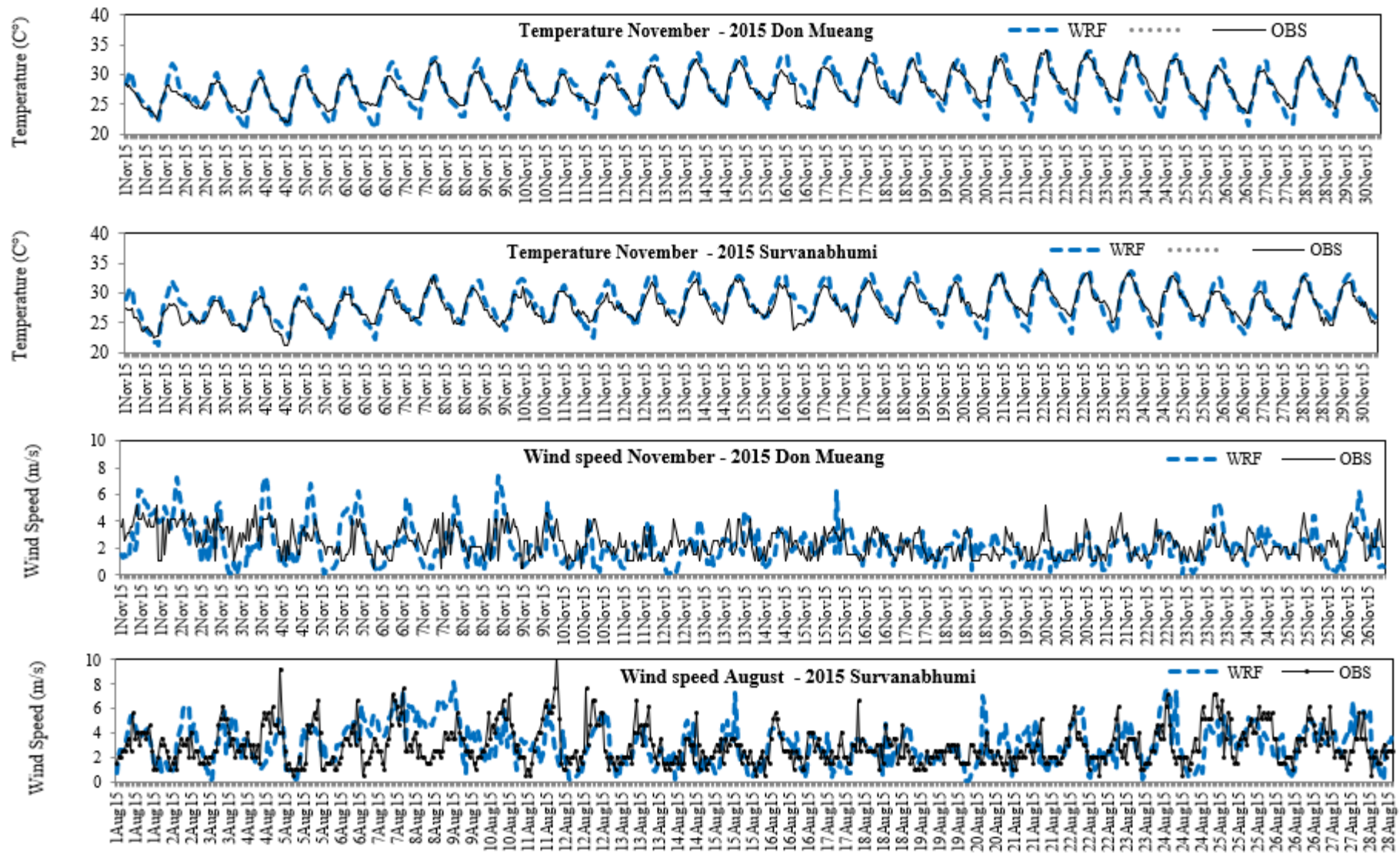
R_1 & R_2 (N): Number of samples measured and calculated both R_1 and R_2

R_1 & R_2 (AA): Number of samples within allowable ranges for both R_1 and R_2

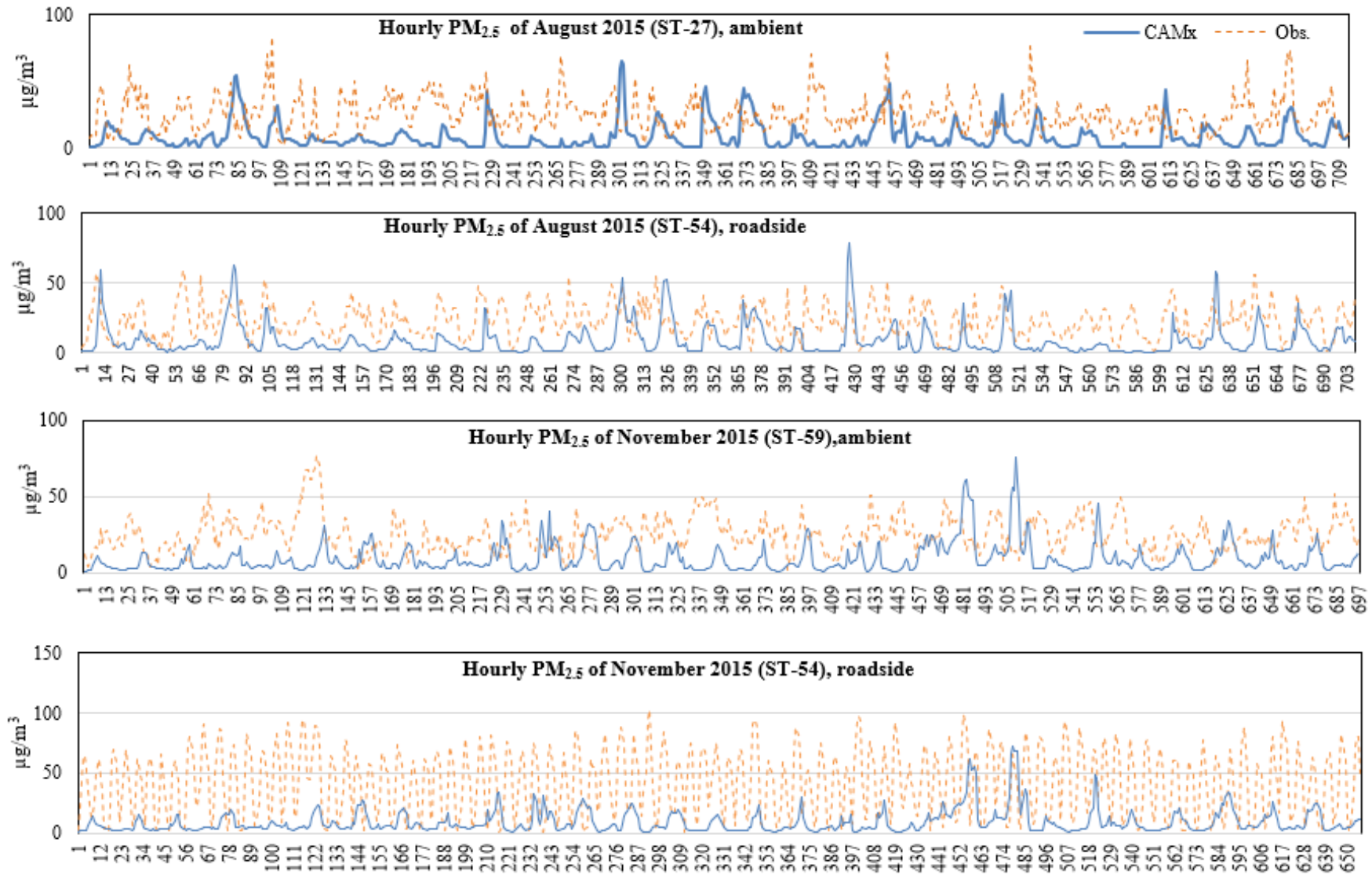
Appendix 10 Monthly average deposition velocity calculated using resistance model provided by ACAP



Appendix 11 Time series of simulated vs observed temperature and wind speed



Appendix 12.1 Time series of simulated vs observed PM_{2.5}



Appendix 12.2 Time series of simulated vs observed PM₁₀

